

SensorLM: Learning the Language of Wearable Sensors

Yuwei Zhang^{1*}, Kumar Ayush^{1*}, Siyuan Qiao², A. Ali Heydari¹, Girish Narayanswamy¹, Maxwell A. Xu¹, Ahmed A. Metwally¹, Shawn Xu¹, Jake Garrison¹, Xuhai Xu¹, Tim Althoff¹, Yun Liu¹, Pushmeet Kohli², Jiening Zhan¹, Mark Malhotra¹, Shwetak Patel¹, Cecilia Mascolo³, Xin Liu¹, Daniel McDuff¹, Yuzhe Yang¹

¹Google Research, ²Google DeepMind, ³University of Cambridge

We present SensorLM, a family of sensor-language foundation models that enable wearable sensor data understanding with natural language. Despite its pervasive nature, aligning and interpreting sensor data with language remains challenging due to the lack of paired, richly annotated sensor-text descriptions in uncurated, real-world wearable data. We introduce a hierarchical caption generation pipeline designed to capture *statistical*, *structural*, and *semantic* information from sensor data. This approach enabled the curation of the largest sensor-language dataset to date, comprising over 59.7 million hours of data from more than 103,000 people. Furthermore, SensorLM extends prominent multimodal pretraining architectures (e.g., CLIP, CoCa) and recovers them as specific variants within a generic architecture. Extensive experiments on real-world tasks in human activity analysis and healthcare verify the superior performance of SensorLM over state-of-the-art in zero-shot recognition, few-shot learning, and cross-modal retrieval. SensorLM also demonstrates intriguing capabilities including scaling behaviors, label efficiency, sensor captioning, and zero-shot generalization to unseen tasks.

1. Introduction

The human experience unfolds as a continuous dialogue between *sensory perception* and *language articulation*. A perceived change in raw physiological readings like “*heart rate*”, can be seamlessly translated from low-level statistical descriptions (e.g., “*heart rate spikes from 65 to 90*”) to high-level semantic abstractions (e.g., “*periods of strength training noted*”). This intrinsic interplay between raw sensation and linguistic abstraction forms human comprehension of internal states, health conditions, behavioral changes, and more [7, 16]. Wearable sensors now record these narratives at unprecedented resolution, producing *minute-level* data that captures dense insights into an individual’s physiological and behavioral states [23, 40]. Aligning and interpreting this rich, continuous stream of fine-grained sensor data with intuitive and actionable language descriptions is critical for user engagement [39], clinical decision-making [37], personalized insights [7], and behavioral interventions [25].

However, directly interpreting continuous raw sensor data poses significant challenges. While large language models (LLMs) excel at processing textual sequences, they inherently struggle with the high-dimensional, continuous, and temporally extensive nature of wearable data [21]. For example, a single day of minute-level multimodal sensor recordings (see Fig. 1(a)) would expand to over 200,000 tokens [23], far exceeding the practical context length limits of most contemporary LLMs [29, 31]. Interestingly, even with minimal subsampling to fit within context constraints, LLMs fail to perform well: Fig. 1(d) illustrates the poor zero-shot performance of Gemma-3-27B [29] and Gemini 2.0 [28] (details in Sec. 5). As such, standard LLM methods either become overwhelmed by data volume or sacrifice the granularity needed for aligning sensor events with meaningful linguistic descriptions.

Furthermore, despite preliminary efforts in constructing paired sensor-text datasets to facilitate effective cross-modal alignment, the absence of *large-scale, high-quality* sensor-language corpora remains a significant bottleneck [6, 10, 15, 39]. As illustrated in Table 1, current sensor-text datasets

*Co-first authors. Work done when Yuwei Zhang interned at Google. Correspondence to: {kmrayush, yuzheyang}@google.com.
© 2025 Google. All rights reserved

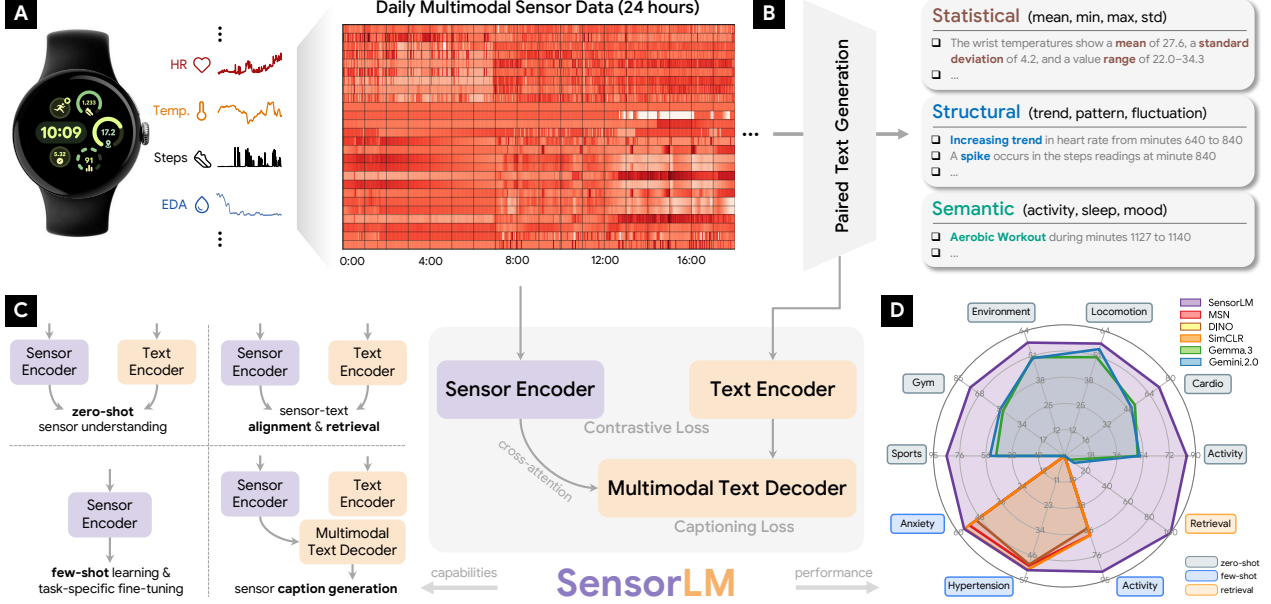


Figure 1 | Sensor-language foundation models (SensorLM) for wearable data. Aligning and interpreting sensor data with natural language remains challenging. (A) We present a comprehensive study using over 59.7 million hours of multimodal wearable data from over 103,000 individuals. (B) We design a hierarchical pipeline for automatic paired text generation that covers **statistical**, **structural**, and **semantic** sensor information. (C) The SensorLM pretraining framework and its use cases for diverse downstream tasks. (D) Radar plot comparing the performance of SensorLM and baselines across various tasks and settings (details in Sec. 5).

are significantly limited in scale and primarily structured in restrictive question-answering formats [6, 15, 39]. This highlights a fundamental gap – the lack of principled and scalable methods for generating truly large-scale and diverse sensor-language datasets. Consequently, existing approaches yield sparse and narrowly scoped sensor-text pairs, insufficient for training generalizable foundation models capable of comprehensive multimodal understanding across diverse, open-ended tasks.

To fill the gap, we introduce **SensorLM**, a family of sensor-language foundation models that unlock meaningful interpretation of raw wearable data and enable novel sensor applications through natural language. The effectiveness of SensorLM stems from three innovations: (1) a hierarchical, automated caption-generation pipeline that systematically captures multi-level features—*statistical*, *structural*, and *semantic*—from fine-grained sensor streams; (2) building upon this pipeline, the curation of the largest-scale sensor-language dataset to date, comprising over 59 million hours of wearable data from more than 103,000 individuals; and (3) a generic pretraining framework that integrates diverse multimodal architectures (e.g., CLIP [24], Cap [32], CoCa [38]) for scalable and robust learning.

To rigorously evaluate SensorLM, we benchmark its performance against state-of-the-art (SOTA) methods across a diverse range of real-world tasks in domains such as human activity analysis and metabolic health. Extensive experiments verify the efficacy of SensorLM on multimodal understanding and its ability to enable new sensor-driven applications. Our contributions are as follows:

- We introduce a hierarchical captioning pipeline for raw sensor data, enabling the curation of the largest sensor-language study to date with over 59 million hours of data from over 103,000 people.
- We design SensorLM, a family of sensor-language foundation models that enable diverse sensor capabilities through natural language.
- We conduct extensive experiments across various tasks in *human activity analysis* and *metabolic health*, verifying the superior performance of SensorLM against SOTA methods.

Table 1 | Comparisons of studies on sensor-text modeling.

Study	# People	# Hours (000s)	Sensors [†]					Text		
			PPG	ACC	EDA	TEMP	ALT	statistical	structural	semantic
Xing <i>et al.</i> [35]	4	<<1	✗	✓	✗	✗	✗	✗	✗	✓
Moon <i>et al.</i> [22]	60	<1	✗	✓	✗	✗	✗	✗	✗	✓
Yu <i>et al.</i> [39]	60	5	✗	✓	✗	✗	✗	✗	✗	✓
Li <i>et al.</i> [15]	214	3.7	✗	✓	✗	✗	✗	✗	✓	✓
SensorLM (ours)	103,731	59,749	✓	✓	✓	✓	✓	✓	✓	✓

[†] PPG: Photoplethysmography. ACC: Accelerometer. EDA: Electrodermal Activity. TEMP: Temperature. ALT: Altitude.

- Further analyses reveal intriguing properties of SensorLM on its scaling behaviors, data efficiency, multimodal understanding & generation, and zero-shot generalization to unseen tasks and concepts.

2. Related Work

Aligning Sensor with Language. Despite growing interests in integrating sensor data with natural language, large-scale paired corpora derived from uncurated wearable data remain scarce, yet are crucial for training effective cross-modal models [24, 34, 38]. Prior work typically addresses this integration by using pre-derived textual summaries of sensor features or ingesting raw sensor values as tabular inputs to LLMs in downstream prediction tasks [7, 13, 16, 20]. Other multimodal methods incorporate specialized sensor encoders with alignment modules to enhance an LLM’s capability to interpret sensor data [6, 10, 14]. Recent efforts initiate the creation of sensor-text data primarily through employing sensor question-answering frameworks [15, 39], explicitly tailored towards human activity recognition. However, these approaches often rely on manual summarization and are inherently limited by sparse and narrowly-scoped sensor-text pairs, restricting generalization to broader scenarios (see Table 1). In contrast, we focus on learning *aligned* sensor-language representations directly from *large-scale, hierarchical* captions, enabling strong zero-shot generalization across diverse tasks.

Multimodal Sensor Foundation Models. Recent advances in sensor data modeling have demonstrated improved accuracy, robustness, and generalization by leveraging self-supervised pretraining on large-scale physiological and wearable sensor datasets [23, 40]. Existing sensor foundation models primarily focus on single-modal but multi-channel sensor data, utilizing either contrastive-based [1, 30, 36, 40] or reconstruction-based pretraining objectives [23]. More recent efforts have explored multimodal sensor foundation models by aligning individual physiological signals (e.g., ECG, EEG) or IMU sensor data with other modalities, including language or vision, through joint representation learning [11, 22, 43]. Our work extends sensor foundation models towards comprehensive *multimodal sensor-language* understanding, enabling novel sensor applications (see Fig. 1) and *multimodal* capabilities via joint modeling of diverse sensor types and natural language.

Vision-Language Pretraining. Vision-language pretraining (VLP) has significantly advanced multimodal AI, enabling models to effectively learn representations that integrate visual and textual data [24, 38]. Leveraging large-scale image-text datasets, VLP methods have produced multimodal foundation models capable of strong zero-shot image classification, captioning, visual question answering, and cross-modal retrieval [24, 34, 38]. Key VLP methods include contrastive learning (e.g., CLIP [24]), which aligns image and text embeddings while separating dissimilar pairs, and generative pretraining (e.g., SimVLM [34]), which employs a prefix language modeling objective. More recent models like CoCa [38] combine both contrastive and generative objectives for enhanced multimodal

performance. The success of VLP has inspired similar pretraining strategies in other modalities such as video, audio, time series [8, 22, 42], as well as specialized domains such as medicine [9, 19, 44]. Our work extends VLP paradigms to the *sensor domain*, implementing a generic pretraining framework that incorporates prominent multimodal architectures for scalable sensor-language modeling.

3. Sensor-Language Dataset Construction

Building a sensor-language foundation model requires two essential components: (1) a large-scale, diverse collection of *sensor data*, and (2) corresponding *captions* that capture useful properties of the data. We summarize prior efforts on sensor-text modeling in Table 1, and detail our study below.

3.1. Sensor Data and Processing

We collected wrist-worn wearable sensor data from Fitbit and Pixel Watch devices. The dataset includes multimodal time series signals from photoplethysmography (PPG), 3-axis accelerometer (ACC), altimeter (ALT), skin temperature (TEMP), and electrodermal activity (EDA) sensors. From these time series, we extracted 26 features: twelve metrics related to heart rate and heart rate variability (HRV) derived from the PPG signal, ten accelerometer-based features (e.g., jerk, steps), as well as the mean and slope of skin temperature, mean tonic electrodermal activity, and mean altimeter pressure (full details are in Appendix A.1). The input to the model consists of one-day windows of sensor data at minutely resolution, resulting in input matrices of shape [26 features \times 1440 minutes].

3.2. Hierarchical Sensor Caption Generation

A significant challenge in sensor-language pretraining is the general absence of paired textual descriptions for wearable sensor data. Unlike domains such as vision or clinical imaging, where data often comes with associated text (e.g., image captions or clinical reports) [9, 24, 38], sensor data collected in the wild typically lacks such naturally occurring pairings. Existing annotations, when available, are often sparse and limited to coarse labels such as discrete activity categories (Table 1).

To bridge this gap and enable robust alignment between natural language and multimodal sensor streams, we propose a *hierarchical* caption generation strategy. This approach creates captions at three distinct levels of abstraction—statistical, structural, and semantic. By doing so, we aim to train a model capable of representing not only basic numerical summaries and dynamic temporal patterns, but also high-level events and contextual states observed in daily sensor data. An illustrative example of the overall process and all three level of captions is shown in Fig. 2.

Statistical Captions. Statistical captions provide a quantitative summary of the sensor data. For each distinct sensor feature channel (e.g., heart rate, temperature, step count), basic statistical measures—including *mean*, *maximum*, *minimum*, and *standard deviation*—are computed. To enhance linguistic diversity, these values are embedded into a variety of sentence structures using a set of templates (details in Appendix A.2). This offers a concise, data-driven overview of individual sensor streams.

Structural Captions. Structural captions focus on encoding the dynamic characteristics and patterns within time-series sensor data. This includes identifying and describing notable *trends*, *fluctuations*, and other *temporal features* across sensor channels. Methodologically, we apply sliding windows to each time series to detect significant increasing, decreasing, or stable trends, as well as identifying sharp spikes and drops. Similar to statistical captions, these identified patterns are then verbalized using a diverse set of templates, from which a random subset is selected for each data sample. This

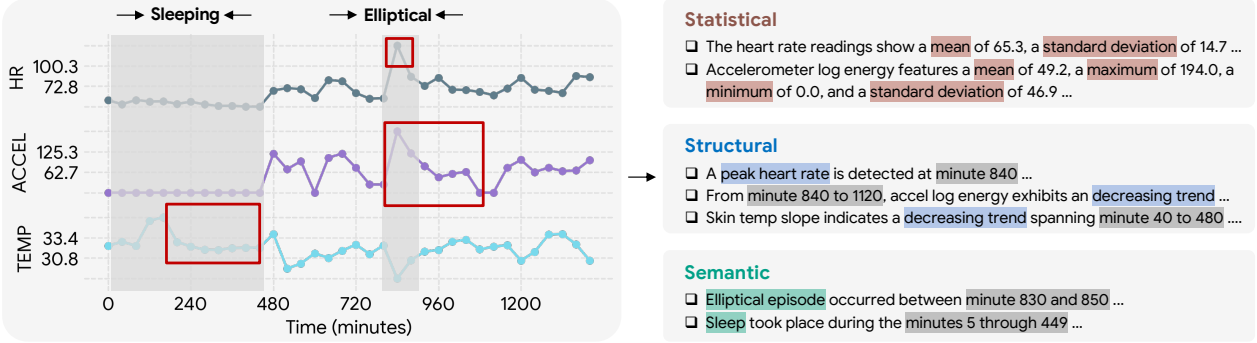


Figure 2 | **Hierarchical sensor caption generation pipeline.** Given multimodal wearable data, we generate three levels of captions: (1) *statistical*, capturing basic quantitative metrics; (2) *structural*, describing temporal patterns, trends, and signal dynamics; and (3) *semantic*, providing contextual information such as behavioral states or physical activity. When applicable, each caption is annotated with its time frame (marked in grey).

enables the model to learn the temporal shape and behavioral dynamics of the sensor signals.

Semantic Captions. Semantic captions aim to capture the high-level meaning and context embedded in the sensor data, reflecting what the individual might be doing or experiencing. This layer incorporates information about recognized activities and sleep periods, specifying start and end times of each event—e.g., “*Observed Outdoor Bike activity from minute 550 to 561*”. Additionally, user-logged mood data with corresponding timestamps is integrated, such as “*The person logged their mood as Frustrated at minute 1110*.“ Integrating this contextual information enables the model to associate real-world events and subjective states with underlying sensor patterns.

3.3. Large-Scale Pretraining Sensor-Text Dataset

Building upon the collected sensor data and caption generation pipeline, we construct the largest sensor-language paired pretraining dataset to date – **orders of magnitude** larger than prior studies (Table 1). All data are de-identified and used with participant consent and IRB review (Advarra). The dataset comprises 2,489,570 person-days of data from 103,643 people across 127 countries, collected between March 1st and May 1st, 2024. (Further details are provided in Appendix A.1.)

We generate multiple caption combinations and evaluate their effectiveness in Sec. 5. Unless otherwise specified, we use the combination of structural and semantic captions in our main experiments.

4. SensorLM

SensorLM presents a generic framework for training sensor-language foundation models (Fig. 3). Inspired by prominent VLP architectures with contrastive (e.g., CLIP [24]), generative (e.g., Cap [32]), and hybrid (e.g., CoCa [38]) objectives, SensorLM extends these approaches to sensor data and recovers them as specific configurations within a single architecture.

From Unimodal to Multimodal Paradigms. We first position SensorLM within the broader family of foundation models that leverage language supervision, adapting these paradigms to the sensor domain. Traditional discriminative single-encoder models perform well on fixed-vocabulary tasks like activity recognition but lack flexibility for open-ended language grounding. Contrastive dual-encoder approaches [24] enable zero-shot generalization and efficient retrieval by aligning modalities in a shared space. Encoder-decoder architectures, in contrast, generate rich natural language conditioned on the input (e.g., sensor data), offering fine-grained interpretability via language. While expressive,

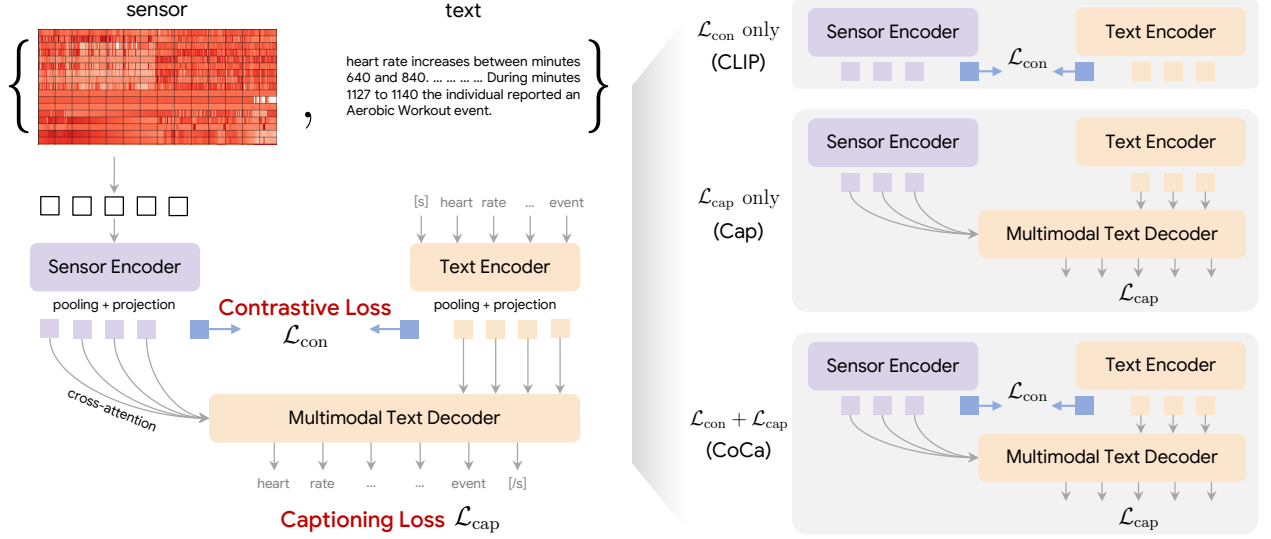


Figure 3 | The SensorLM architecture, pretraining objectives, and representative variants. Our framework integrates both contrastive (\mathcal{L}_{con}) and generative (\mathcal{L}_{cap}) objectives, extending prior approaches (e.g., CLIP [24], Cap [32], CoCa [38]) to sensor data and recovering them as specific configurations within a single architecture.

they may struggle with robust cross-modal alignment. SensorLM integrates these complementary strategies into a single framework for sensor-language pretraining.

Architecture. SensorLM comprises a sensor encoder, a text encoder, and a multimodal text decoder (Fig. 3). The *sensor encoder* transforms time-series sensor data into a compact latent representations. We adapt a Vision Transformer (ViT) architecture to handle sensor data by segmenting the sequence into patches, applying linear embeddings, and processing them through transformer blocks to capture both local and long-range temporal dependencies. The *text encoder* follows a similar process to encode input text into unimodal representations. Finally, the *multimodal text decoder* is a causally masked transformer that integrates both sensor features (via cross-attention) and text features to produce multimodal text representations.

Pretraining Objectives. SensorLM is pretrained with a composite loss function that combines both *contrastive* and *generative* objectives. Given a batch of N sensor-text pairs $\{(x_n, y_n)\}_{n \in [N]}$, the *contrastive loss* \mathcal{L}_{con} is applied to normalized unimodal text embeddings v_i (from the text encoder) and sensor embeddings s_i (from the sensor encoder) via a symmetric cross-modal objective [5]:

$$\mathcal{L}_{\text{con}} = -\frac{1}{N} \left(\underbrace{\sum_{i=1}^N \log \frac{\exp(\text{sim}(s_i, v_i)/\tau)}{\sum_{j=1, j \neq i}^N \exp(\text{sim}(s_i, v_j)/\tau)} + \sum_{i=1}^N \log \frac{\exp(\text{sim}(v_i, s_i)/\tau)}{\sum_{j=1, j \neq i}^N \exp(\text{sim}(v_i, s_j)/\tau)} \right),$$

where $\text{sim}(\cdot, \cdot)$ is the similarity measure between embeddings, and τ denotes the temperature parameter. The *captioning loss* \mathcal{L}_{cap} is a standard cross-entropy loss applied to the outputs of multimodal text decoder. It maximizes the conditional likelihood of the paired text y given the sensor input x under a forward autoregressive factorization:

$$\mathcal{L}_{\text{cap}} = - \sum_{t=1}^T \log \mathbb{P}_\theta(y_t | y_{<t}, x).$$

Combined Objective and Representative Variants. The final objective is a weighted combination: $\mathcal{L}_{\text{SensorLM}} = \lambda_{\text{con}} \cdot \mathcal{L}_{\text{con}} + \lambda_{\text{cap}} \cdot \mathcal{L}_{\text{cap}}$, where λ_{con} and λ_{cap} control the balance between contrastive and generative learning. Under this unified formulation, SensorLM seamlessly recovers representative

variants within a single framework (Fig. 3): (1) CLIP (i.e., $\lambda_{\text{cap}} = 0$), (2) Cap (i.e., $\lambda_{\text{con}} = 0$), and (3) CoCa (i.e., $\lambda_{\text{con}} = \lambda_{\text{cap}} = 1$). We investigate these model variants in Sec. 5.3.

The SensorLM Family. We train four variants of SensorLM with increasing sizes: SensorLM-S, SensorLM-B, SensorLM-L, and SensorLM-XL. These variants employ sensor encoders with 3M, 114M, 404M, and 1.27B parameters (details in Appendix B.1). We study the effects of model scaling in Sec. 5 and Appendix C.1. Unless otherwise specified, we report results using SensorLM-B.

5. Experiments & Results

Datasets. We utilize three evaluation datasets for activity recognition, health-related tasks and cross-modal retrieval. Detailed information and demographic breakdowns are provided in Appendix A.3.

- **Activity dataset.** The Activity dataset comprises 22,289 person-days from 10,013 individuals. We randomly sampled ~1,000 test examples for each activity for zero-shot activity recognition (AR) and few-shot adaptation. This dataset is from the same population as our pretraining sensor data.
- **Metabolic dataset.** The metabolic dataset, used for “Hypertension” and “Anxiety” prediction tasks, were sourced from a held-out, IRB-approved observational study of adults in the US. The data comprises 241,532 examples (151,346 training and 90,186 testing) from 1,979 individuals. It includes self-reported information covering demographics (e.g., age, sex, weight) and medical conditions (e.g., “Hypertension” and “Anxiety”), providing rich labels for health analyses.
- **Sensor-text retrieval dataset.** We construct a retrieval dataset of 39,766 examples sourced from a separate set of 975 individuals who were not included in the pretraining set. The same selection criteria and caption generation method used in pretraining were applied.

Baselines. For zero-shot classification and cross-modal retrieval, there are currently no existing multimodal baselines with these capabilities. We therefore compare against two LLMs, Gemini 2.0 Flash [28] and Gemma-3-27B [29], by formatting sensor data as tabular input. For few-shot learning and linear probing, we compare with SOTA SSL methods including SimCLR [5], DINO [3], and Masked Siamese Network (MSN) [2]. Implementation details can be found in Appendix B.

Metrics. For zero-shot classification, we report area under the ROC curve (AUROC), Macro F1-score, and Balanced Accuracy (BAcc). For few-shot learning, we report AUROC across 5, 10, 20, 50 samples per class. Cross-modal retrieval is evaluated using Recall@1 and Recall@5 (R@K).

5.1. Main Results

Zero-Shot Learning. One of the key capabilities enabled by SensorLM is zero-shot classification, which we evaluate on a range of AR tasks. We use prompt ensembling [24] from the text encoder with diverse prompts to compute average label embeddings, and classify by selecting the label whose embedding is closest to the sensor embedding. We include 6 tasks in total, including *20-class activity recognition*, *activity concept classification* (2-4 classes by “environmental” context or “physiological” type), and *fine-grained recognition* (4 classes within “gym cardio” or “outdoor sports”). As shown in Table 2, LLM baselines perform near random on sensor-based activity classification. In contrast, SensorLM demonstrates strong zero-shot capabilities across all metrics and tasks. For abstract concepts such as “environmental” or “physiological” type, the superior performance suggests that the model captures both explicit activity categories and *higher-level conceptual understanding*.

Table 2 | Zero-shot activity and concept classification. We compare SensorLM with representative LLM baselines across **(a)** main activity classification, **(b-d)** activity-related concept classification, and **(e-f)** fine-grained recognition. Detailed task definitions and experimental setups are provided in Appendix B.5.

(a) Activity recognition (20-class)

Metrics	AUROC \uparrow	F1 \uparrow	BAcc \uparrow
Gemma-3-27B [29]	0.50	0.01	0.05
Gemini 2.0 [28]	0.51	0.03	0.07
SensorLM	0.84 (+33%)	0.29 (+26%)	0.31 (+24%)

(b) Activity by environmental context

Metrics	AUROC \uparrow	F1 \uparrow	BAcc \uparrow
Gemma-3-27B [29]	0.51	0.22	0.25
Gemini 2.0 [28]	0.50	0.19	0.25
SensorLM	0.64 (+13%)	0.33 (+11%)	0.38 (+13%)

(c) Cardio vs. strength training

Metrics	AUROC \uparrow	F1 \uparrow	BAcc \uparrow
Gemma-3-27B [29]	0.53	0.42	0.49
Gemini 2.0 [28]	0.50	0.39	0.50
SensorLM	0.71 (+18%)	0.63 (+21%)	0.66 (+16%)

(d) Locomotion vs. stationary

Metrics	AUROC \uparrow	F1 \uparrow	BAcc \uparrow
Gemma-3-27B [29]	0.51	0.40	0.51
Gemini 2.0 [28]	0.55	0.52	0.55
SensorLM	0.61 (+06%)	0.58 (+06%)	0.58 (+03%)

(e) Fine-grained recognition (gym cardio)

Metrics	AUROC \uparrow	F1 \uparrow	BAcc \uparrow
Gemma-3-27B [29]	0.49	0.16	0.25
Gemini 2.0 [28]	0.52	0.20	0.26
SensorLM	0.76 (+24%)	0.50 (+30%)	0.51 (+25%)

(f) Fine-grained recognition (outdoor sports)

Metrics	AUROC \uparrow	F1 \uparrow	BAcc \uparrow
Gemma-3-27B [29]	0.50	0.18	0.25
Gemini 2.0 [28]	0.54	0.22	0.29
SensorLM	0.83 (+29%)	0.52 (+30%)	0.53 (+24%)

Zero-Shot Cross-Modal Retrieval. We evaluate the zero-shot cross-modal retrieval performance of SensorLM by assessing its ability to retrieve relevant text descriptions given sensor queries ($\text{Sensor} \rightarrow \text{Text}$) and vice versa ($\text{Text} \rightarrow \text{Sensor}$). Sensor-to-text retrieval enables querying description based on sensor input, while text-to-sensor retrieval supports use cases such as expert-driven querying for specific sensor patterns using natural language. Table 3 confirms SensorLM’s exceptionally strong performance across all sample sizes, significantly outperforming LLM baselines, which largely failed at this task. SensorLM achieves perfect retrieval on a 100-sample benchmark and maintains high accuracy even at larger scales (5k and 40k samples; full results in Appendix C.3).

Qualitatively, Fig. 4 verifies SensorLM’s ability to retrieve accurate descriptions for unseen sensor data involving multiple activities. In addition to correctly retrieving the ground truth, the top similar captions are also semantically relevant – capturing either similar activities occurring at the same time (e.g., “Walk” vs. “Run”) or the same activity at different times. This reflects its understanding of both activity semantics and temporal alignment.

Few-Shot Transfer Learning. We evaluate the quality of the learned sensor representations through few-shot learning on three tasks: 20-class AR using the *Activity* dataset, and two binary prediction tasks on clinical condition (“Hypertension”) and mental health (“Anxiety”) using the *Metabolic* dataset. Fig. 5 shows the few-shot performance of SensorLM compared to baseline SSL methods as the number of training labels per class increases from 5 to 50. For AR, SensorLM significantly

Table 3 | Zero-shot cross-modal retrieval. SensorLM achieves consistently strong retrieval performance on a held-out dataset. Baseline LLMs struggle, with most tasks infeasible due to context limits (marked as “–”). Detailed experimental setups and complete results are in Appendix B.7 and C.3.

Metrics	100 samples		5,000 samples	
	R@1	R@5	R@1	R@5
<i>Sensor → Text:</i>				
Gemma-3-27B [29]	1.0	5.0	–	–
Gemini 2.0 [28]	5.0	9.0	–	–
SensorLM	100.0	100.0	98.2	99.4
<i>Text → Sensor:</i>				
Gemma-3-27B [29]	–	–	–	–
Gemini 2.0 [28]	–	–	–	–
SensorLM	100.0	100.0	96.7	99.2

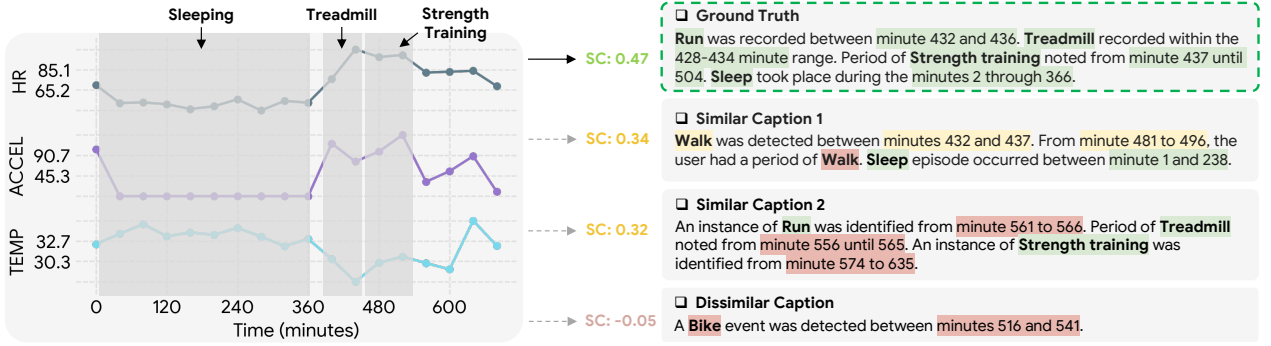


Figure 4 | Zero-shot sensor-to-text retrieval qualitative example. We show similarity scores (SC) for the correctly retrieved ground truth, top similar captions, and a dissimilar caption. Green highlights correct events and time frames; Yellow indicates partial matches; and Red denotes incorrect events and time frames. In addition to correctly retrieving the ground truth, SensorLM also demonstrates semantic understanding by assigning high similarity scores to partially correct candidates.

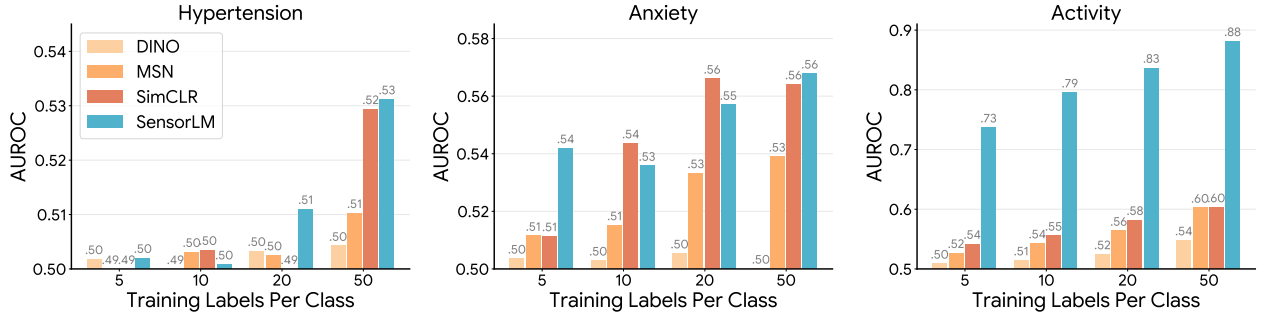


Figure 5 | Few-shot adaptation to downstream tasks. We evaluate the label efficiency of different pretrained sensor encoders with varying numbers of training labels per class. Across diverse tasks, SensorLM achieves comparable or superior performance than SOTA methods. Additional results are provided in Appendix C.2.

outperforms baselines across all few-shot settings, achieving an AUROC of 0.88 with only 50 labels per class, highlighting its effective representations in discriminating activities under limited supervision. For “Hypertension” and “Anxiety” prediction, SensorLM shows competitive performance. Linear probing results on the full training set support similar conclusions (Appendix C.2).

5.2. Analyses

Scaling Laws (Appendix C.1). We investigate the scaling behavior of SensorLM when trained on large-scale sensor-language dataset by varying *training compute*, *dataset size*, and *model scale* [12]. We observe that performance on zero-shot activity recognition improves consistently with increased training steps and data size, though gains beyond 12 million hours show diminishing returns for certain models, which has been observed in prior work [12, 23]. Larger models generally outperform smaller ones when adequately trained, but undertraining can lead to degraded performance, as observed with SensorLM-XL at low compute. These trends suggest that scaling laws observed in other domains also hold in sensor-language modeling.

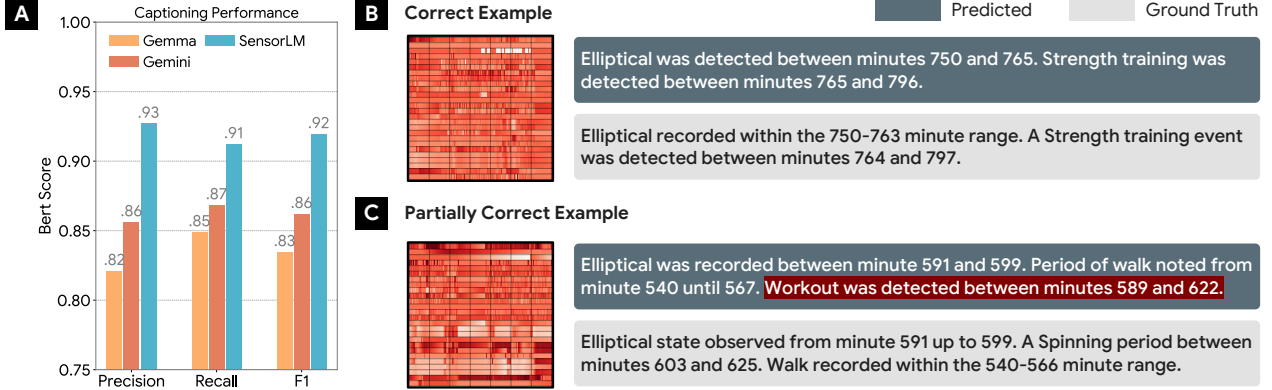


Figure 7 | Sensor caption generation results. (A) Captioning performance of SensorLM and baselines. For SensorLM, only the sensor data and a [START] token are provided to generate captions. (B) A correctly generated example. (C) A partially correct example with inaccurate components. SensorLM produces meaningful and semantically accurate captions. Detailed experimental setups and additional results are in Appendix B.9 and C.4.

Zero-Shot Generalization to Unseen Classes. To evaluate SensorLM’s generalizability to novel activities, we conducted a case study by pre-training on data comprising 20 activity classes and tested on previously unseen ones (details in Appendix B.8). The results of one-versus-all AUROC and 95% CIs for these classes are shown in Fig. 6(a). The impressive zero-shot performance achieved on these unseen activities indicates that SensorLM learns the broader concept of activities rather than memorizing the training set. Specifically, activities that are conceptually similar to those in the training set exhibit higher performance (e.g., “Snowboarding” is similar to “Skiing”). This is further supported by the visualization of label and sensor embeddings using t-SNE [33] (Fig. 6(b)), where semantically related activities form coherent clusters, indicating that SensorLM infers unseen classes based on their proximity to known concepts in the learned embedding space.

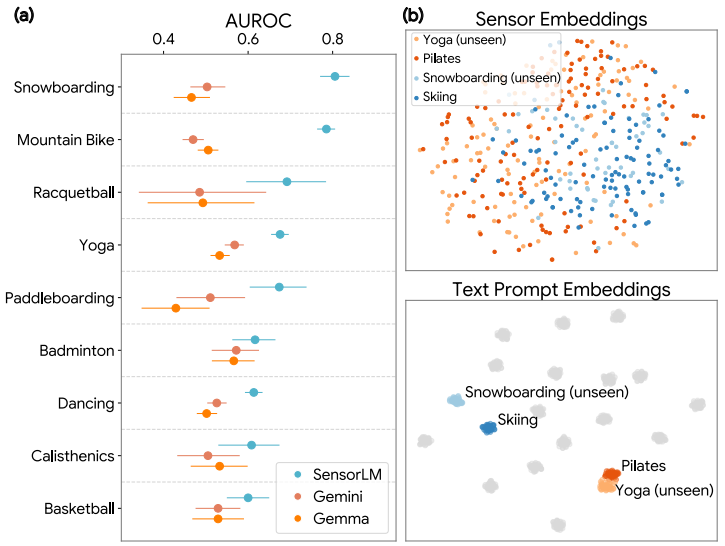


Figure 6 | Zero-shot generalization analysis of SensorLM. (a) Overall performance on unseen activities. (b) Learned representations in both the sensor and text embedding spaces. We visualize conceptually similar but previously unseen activities as a case study. The semantic alignment across modalities allows SensorLM to infer the nature of unseen activities based on their conceptual proximity to known ones.

Sensor Caption Generation. A key strength of SensorLM stems from its encoder-decoder architecture, trained with a generative objective. This design positions SensorLM to effectively process multimodal sensor embeddings, yielding *sensor captioning* capabilities. Beyond its inherent classification and retrieval capabilities, SensorLM demonstrates strong generative performance. On a dedicated evaluation set of 200 sensor-text pairs (sampled from the sensor-caption retrieval dataset), SensorLM directly generates captions from sensor input (and a [START] token). As shown in Fig. 7, SensorLM (pre-trained on semantic captions) outperforms powerful LLM baselines, including

Gemini 2.0 Flash [28] and Gemma-3-27B [29]. These results highlight SensorLM’s capability as a sensor-language foundation model that can both interpret sensor data and generate meaningful natural language descriptions.

5.3. Ablation Studies

Understanding the impact of pretraining caption variants. We investigate how different levels of sensor descriptions affect downstream tasks. Table 4 shows that semantic captions are crucial for zero-shot AR, whereas models trained solely on statistical or structural captions underperform due to a lack of activity-level concepts. Combining semantic and structural captions improves zero-shot AR over semantic-only models, indicating that local signal patterns and temporal structure contribute complementary information. However, adding statistical captions to semantic ones reduces zero-shot AR performance, likely because daily-level statistics are less relevant to fine-grained activities. Yet, statistical captions benefit “Anxiety” and “Hypertension” predictions, either alone or when combined with other caption types. Overall, the “semantic + structural” combination provides the best trade-off across tasks.

Pretraining architectural variants. We study different architectural variants trained with contrastive and generative objectives. As Table 5 reports, SensorLM (CoCa) consistently outperforms the single-objective variants across key metrics for both zero-shot classification and linear probing. The generative objective enhances the contrastive alignment by providing fine-grained text supervision, leading to improved cross-modal understanding. Notably, the SensorLM (Cap) model performs poorly in zero-shot classification due to the absence of a trained projection head.

6. Discussion

Limitations. It is crucial to understand that SensorLM is not a clinically validated diagnostic tool and is not intended for clinical diagnosis, treatment, or medical decision-making; deployment for such uses would require further analysis of applicable healthcare regulations. Additionally, our evaluation is limited to specific wearable devices and sensor data; while the method is general, further work is needed to explore its generalizability on other types of sensor data.

Conclusion. We present SensorLM, a family of sensor-language foundation models that unlock the understanding of wearable sensor data through natural language, enabled by a novel hierarchical captioning pipeline and the largest sensor-language dataset to date. SensorLM achieves superior performance in zero-shot, few-shot, and cross-modal retrieval tasks, as well as demonstrating intriguing properties such as scaling, generative, and zero-shot generalization capabilities.

Table 4 | Comparisons of SensorLM caption variants. We evaluate different combinations of caption types used during pretraining. AUROC \uparrow is used as the metric. Best results of each column are in **bold** and the second best are underlined. Default setting used in the main experiments is marked in gray .

Caption Variant				Zero-Shot	Linear Probing
	statistical	structural	semantic	Activity	Activity Anxiety
✓	✗	✗	✗	0.51	0.76 0.67
✗	✓	✗	✗	0.50	0.78 0.63
✗	✗	✓	✓	<u>0.71</u>	0.95 0.65
✓	✗	✓	✓	0.66	0.84 0.68
✗	✓	✓	✓	0.84	<u>0.94</u> 0.65
✓	✓	✗	✗	0.49	0.79 0.67
✓	✓	✓	✓	0.66	0.86 0.68

Table 5 | Comparisons of SensorLM architectural variants. We compare different choices used during pretraining. Default setting used in the main experiments is marked in gray .

Arch Variant	Zero-Shot		Linear Probing	
	AUROC \uparrow	F1 \uparrow	AUROC \uparrow	F1 \uparrow
SensorLM (CLIP)	0.83	0.29	0.93	0.53
SensorLM (Cap)	0.55	0.01	0.90	0.32
SensorLM (CoCa)	0.84	0.29	0.94	0.57

References

- [1] Salar Abbaspourazad, Oussama Elachqar, Andrew Miller, Saba Emrani, Udhayakumar Nallasamy, and Ian Shapiro. Large-scale training of foundation models for wearable biosignals. In *The Twelfth International Conference on Learning Representations*, 2023.
- [2] Mahmoud Assran, Mathilde Caron, Ishan Misra, Piotr Bojanowski, Florian Bordes, Pascal Vincent, Armand Joulin, Mike Rabbat, and Nicolas Ballas. Masked siamese networks for label-efficient learning. In *European Conference on Computer Vision*, pages 456–473. Springer, 2022.
- [3] Mathilde Caron, Hugo Touvron, Ishan Misra, Hervé Jégou, Julien Mairal, Piotr Bojanowski, and Armand Joulin. Emerging properties in self-supervised vision transformers. In *Proceedings of the IEEE/CVF International Conference on Computer Vision*, pages 9650–9660, 2021.
- [4] James Carpenter and John Bithell. Bootstrap confidence intervals: when, which, what? a practical guide for medical statisticians. *Statistics in medicine*, 19(9):1141–1164, 2000.
- [5] Ting Chen, Simon Kornblith, Mohammad Norouzi, and Geoffrey Hinton. A simple framework for contrastive learning of visual representations. In *International conference on machine learning*, pages 1597–1607. PMLR, 2020.
- [6] Wenqiang Chen, Jiaxuan Cheng, Leyao Wang, Wei Zhao, and Wojciech Matusik. Sensor2text: Enabling natural language interactions for daily activity tracking using wearable sensors. *Proceedings of the ACM on Interactive, Mobile, Wearable and Ubiquitous Technologies*, 8(4):1–26, 2024.
- [7] Justin Cosentino, Anastasiya Belyaeva, Xin Liu, Nicholas A Furlotte, Zhun Yang, Chace Lee, Erik Schenck, Yojan Patel, Jian Cui, Logan Douglas Schneider, et al. Towards a personal health large language model. *arXiv preprint arXiv:2406.06474*, 2024.
- [8] Benjamin Elizalde, Soham Deshmukh, Mahmoud Al Ismail, and Huaming Wang. Clap learning audio concepts from natural language supervision. In *ICASSP 2023-2023 IEEE International Conference on Acoustics, Speech and Signal Processing (ICASSP)*, pages 1–5. IEEE, 2023.
- [9] Zhi Huang, Federico Bianchi, Mert Yuksekgonul, Thomas J Montine, and James Zou. A visual-language foundation model for pathology image analysis using medical twitter. *Nature medicine*, 29(9):2307–2316, 2023.
- [10] Sheikh Asif Imran, Mohammad Nur Hossain Khan, Subrata Biswas, and Bashima Islam. Llasa: A multimodal llm for human activity analysis through wearable and smartphone sensors. *arXiv preprint arXiv:2406.14498*, 2024.
- [11] Weibang Jiang, Yansen Wang, Bao-liang Lu, and Dongsheng Li. Neurolm: A universal multi-task foundation model for bridging the gap between language and eeg signals. In *The Thirteenth International Conference on Learning Representations*, 2025.
- [12] Jared Kaplan, Sam McCandlish, Tom Henighan, Tom B Brown, Benjamin Chess, Rewon Child, Scott Gray, Alec Radford, Jeffrey Wu, and Dario Amodei. Scaling laws for neural language models. *arXiv preprint arXiv:2001.08361*, 2020.
- [13] Yubin Kim, Xuhai Xu, Daniel McDuff, Cynthia Breazeal, and Hae Won Park. Health-llm: Large language models for health prediction via wearable sensor data. *arXiv preprint arXiv:2401.06866*, 2024.

- [14] Junnan Li, Dongxu Li, Silvio Savarese, and Steven Hoi. Blip-2: Bootstrapping language-image pre-training with frozen image encoders and large language models. In *International conference on machine learning*, pages 19730–19742. PMLR, 2023.
- [15] Zechen Li, Shohreh Deldari, Linyao Chen, Hao Xue, and Flora D. Salim. SensorLLM: Aligning large language models with motion sensors for human activity recognition, 2025.
- [16] Xin Liu, Daniel McDuff, Geza Kovacs, Isaac Galatzer-Levy, Jacob Sunshine, Jiening Zhan, Ming-Zher Poh, Shun Liao, Paolo Di Achille, and Shwetak Patel. Large language models are few-shot health learners. *arXiv preprint arXiv:2305.15525*, 2023.
- [17] Ziyu Liu, Azadeh Alavi, Minyi Li, and Xiang Zhang. Guidelines for augmentation selection in contrastive learning for time series classification. *arXiv preprint arXiv:2407.09336*, 2024.
- [18] Ilya Loshchilov and Frank Hutter. Decoupled weight decay regularization. *International Conference on Learning Representations*, 2017.
- [19] Ming Y Lu, Bowen Chen, Drew FK Williamson, Richard J Chen, Ivy Liang, Tong Ding, Guillaume Jaume, Igor Odintsov, Long Phi Le, Georg Gerber, et al. A visual-language foundation model for computational pathology. *Nature Medicine*, 30(3):863–874, 2024.
- [20] Mike A Merrill, Akshay Paruchuri, Naghmeh Rezaei, Geza Kovacs, Javier Perez, Yun Liu, Erik Schenck, Nova Hammerquist, Jake Sunshine, Shyam Tailor, et al. Transforming wearable data into health insights using large language model agents. *arXiv preprint arXiv:2406.06464*, 2024.
- [21] Mike A. Merrill, Mingtian Tan, Vinayak Gupta, Thomas Hartvigsen, and Tim Althoff. Language models still struggle to zero-shot reason about time series. In *EMNLP (Findings)*, pages 3512–3533, 2024.
- [22] Seungwhan Moon, Andrea Madotto, Zhaojiang Lin, Aparajita Saraf, Amy Bearman, and Babak Damavandi. Imu2clip: language-grounded motion sensor translation with multimodal contrastive learning. In *Findings of the Association for Computational Linguistics: EMNLP 2023*, pages 13246–13253, 2023.
- [23] Girish Narayanswamy, Xin Liu, Kumar Ayush, Yuzhe Yang, Xuhai Xu, shun liao, Jake Garrison, Shyam A. Tailor, Jacob Sunshine, Yun Liu, Tim Althoff, Shrikanth Narayanan, Pushmeet Kohli, Jiening Zhan, Mark Malhotra, Shwetak Patel, Samy Abdel-Ghaffar, and Daniel McDuff. Scaling wearable foundation models. In *The Thirteenth International Conference on Learning Representations*, 2025.
- [24] Alec Radford, Jong Wook Kim, Chris Hallacy, Aditya Ramesh, Gabriel Goh, Sandhini Agarwal, Girish Sastry, Amanda Askell, Pamela Mishkin, Jack Clark, et al. Learning transferable visual models from natural language supervision. In *International conference on machine learning*, pages 8748–8763. PmLR, 2021.
- [25] Mickael Ringeval, Gerit Wagner, James Denford, Guy Paré, and Spyros Kitsiou. Fitbit-based interventions for healthy lifestyle outcomes: systematic review and meta-analysis. *Journal of medical Internet research*, 22(10):e23954, 2020.
- [26] Cédric Rommel, Joseph Paillard, Thomas Moreau, and Alexandre Gramfort. Data augmentation for learning predictive models on eeg: a systematic comparison. *Journal of Neural Engineering*, 19(6):066020, 2022.
- [27] Chi Ian Tang, Ignacio Perez-Pozuelo, Dimitris Spathis, and Cecilia Mascolo. Exploring contrastive learning in human activity recognition for healthcare. *arXiv preprint arXiv:2011.11542*, 2020.

- [28] Gemini Team, Rohan Anil, Sebastian Borgeaud, Jean-Baptiste Alayrac, Jiahui Yu, Radu Soricut, Johan Schalkwyk, Andrew M Dai, Anja Hauth, Katie Millican, et al. Gemini: a family of highly capable multimodal models. *arXiv preprint arXiv:2312.11805*, 2023.
- [29] Gemma Team, Aishwarya Kamath, Johan Ferret, Shreya Pathak, Nino Vieillard, Ramona Merhej, Sarah Perrin, Tatiana Matejovicova, Alexandre Ramé, Morgane Rivière, et al. Gemma 3 technical report. *arXiv preprint arXiv:2503.19786*, 2025.
- [30] Rahul Thapa, Bryan He, Magnus Ruud Kjaer, Hyatt Moore IV, Gauri Ganjoo, Emmanuel Mignot, and James Zou. SleepFM: Multi-modal representation learning for sleep across brain activity, ECG and respiratory signals. In *Forty-first International Conference on Machine Learning*, 2024.
- [31] Hugo Touvron, Louis Martin, Kevin Stone, Peter Albert, Amjad Almahairi, Yasmine Babaei, Nikolay Bashlykov, Soumya Batra, Prajjwal Bhargava, Shruti Bhosale, et al. Llama 2: Open foundation and fine-tuned chat models. *arXiv preprint arXiv:2307.09288*, 2023.
- [32] Michael Tschannen, Manoj Kumar, Andreas Steiner, Xiaohua Zhai, Neil Houlsby, and Lucas Beyer. Image captioners are scalable vision learners too. *Advances in Neural Information Processing Systems*, 36:46830–46855, 2023.
- [33] Laurens Van der Maaten and Geoffrey Hinton. Visualizing data using t-sne. *Journal of machine learning research*, 9(11), 2008.
- [34] Zirui Wang, Jiahui Yu, Adams Wei Yu, Zihang Dai, Yulia Tsvetkov, and Yuan Cao. Simvlm: Simple visual language model pretraining with weak supervision. *arXiv preprint arXiv:2108.10904*, 2021.
- [35] Tianwei Xing, Luis Garcia, Federico Cerutti, Lance Kaplan, Alun Preece, and Mani Srivastava. Deepsqa: Understanding sensor data via question answering. In *Proceedings of the International Conference on Internet-of-Things Design and Implementation*, pages 106–118, 2021.
- [36] Yuzhe Yang, Xin Liu, Jiang Wu, Silviu Borac, Dina Katabi, Ming-Zher Poh, and Daniel McDuff. Simper: Simple self-supervised learning of periodic targets. In *The Eleventh International Conference on Learning Representations*, 2023.
- [37] Yuzhe Yang, Yuan Yuan, Guo Zhang, Hao Wang, Ying-Cong Chen, Yingcheng Liu, Christopher G Tarolli, Daniel Crepeau, Jan Bukartyk, Mithri R Junna, et al. Artificial intelligence-enabled detection and assessment of parkinson’s disease using nocturnal breathing signals. *Nature Medicine*, 28(10):2207–2215, 2022.
- [38] Jiahui Yu, Zirui Wang, Vijay Vasudevan, Legg Yeung, Mojtaba Seyedhosseini, and Yonghui Wu. Coca: Contrastive captioners are image-text foundation models. *arXiv preprint arXiv:2205.01917*, 2022.
- [39] Xiaofan Yu, Lanxiang Hu, Benjamin Reichman, Dylan Chu, Rushil Chandrupatla, Xiyuan Zhang, Larry Heck, and Tajana Rosing. Sensorchat: Answering qualitative and quantitative questions during long-term multimodal sensor interactions. *arXiv preprint arXiv:2502.02883*, 2025.
- [40] Hang Yuan, Shing Chan, Andrew P Creagh, Catherine Tong, Aidan Acquah, David A Clifton, and Aiden Doherty. Self-supervised learning for human activity recognition using 700,000 person-days of wearable data. *NPJ digital medicine*, 7(1):91, 2024.
- [41] Xiang Zhang, Ziyuan Zhao, Theodoros Tsiligkaridis, and Marinka Zitnik. Self-supervised contrastive pre-training for time series via time-frequency consistency. *Advances in neural information processing systems*, 35:3988–4003, 2022.

- [42] Xiyuan Zhang, Diyan Teng, Ranak Roy Chowdhury, Shuheng Li, Dezhi Hong, Rajesh Gupta, and Jingbo Shang. Unimts: Unified pre-training for motion time series. *Advances in Neural Information Processing Systems*, 37:107469–107493, 2024.
- [43] Yubao Zhao, Tian Zhang, Xu Wang, Puyu Han, Tong Chen, Linlin Huang, Youzhu Jin, and Jiaju Kang. Ecg-chat: A large ecg-language model for cardiac disease diagnosis. *arXiv preprint arXiv:2408.08849*, 2024.
- [44] Yukun Zhou, Mark A Chia, Siegfried K Wagner, Murat S Ayhan, Dominic J Williamson, Robbert R Struyven, Timing Liu, Moucheng Xu, Mateo G Lozano, Peter Woodward-Court, et al. A foundation model for generalizable disease detection from retinal images. *Nature*, 622(7981):156–163, 2023.

A. Dataset Overview

A.1. Pretraining Sensor Dataset

Our wearable devices incorporate five distinct sensors: *Photoplethysmography* (PPG), *Accelerometer* (ACC), *Skin Conductance* (electrodermal activity, EDA), *Skin Temperature* (TEMP), and *Altitude* (ALT). While these sensors collect raw waveform signals at high frequencies (i.e., 100Hz, 25Hz, 200Hz, 6Hz, and 10Hz, respectively), we do not directly utilize these high-resolution signals. This decision is driven by practical constraints, including prohibitive storage requirements and battery consumption, which make raw data storage infeasible at our scale. Moreover, learning from full-day raw waveforms is computationally impractical; for example, a 200Hz signal over 24 hours results in approximately 17 million time points per instance.

Instead, we curate minutely aggregated features from the raw signals and use them as model inputs. These features are grounded in established domain literature, with prior work demonstrating their clinical utility [23]. For example, heart rate variability metrics like *RMSSTD* and the *Shannon Entropy of RR Intervals* are recognized markers of cardiovascular health, while accelerometer-derived features such as *Jerk Ratio* capture movement quality. Descriptions of the derived features and their associated sensor modalities are provided in Table 6.

Table 7 summarizes the demographic composition of our pretraining dataset. The only inclusion criterion was having valid sensor data for at least 20% of one day and at least one logged event. The cohort is 38% female with a mean age of 41.7 years (range: 18 – 100). BMI distributions indicate 37% healthy (< 25), 33% overweight (25 – 30), and 25% obese (≥ 30), with the remaining 5% unspecified.

A.2. Sensor Caption Generation

To encourage linguistic diversity and prevent overfitting to a single text pattern, we employ a variety of sentence templates across the three levels of sensor captions. This section details the design of these templates.

Table 8 provides a selection of **statistical caption** templates, illustrated using “Heart rate” as the example feature with an average of 88.7, standard deviation of 9.3, minimum of 70.8, and maximum of 134.9. We employ 20 rewrite templates in total to generate varied statistical descriptions.

Table 9 shows examples of **structural caption** templates, including descriptions of trends (e.g., “*a decreasing trend in heart rate between minute 680 and 960*”) and spike events (e.g., “*a spike in step count at minute 720*”). We use 15 rewrite templates in total for structural captions.

Table 10 presents templates for **semantic captions**, which describe high-level activities and their associated timeframes, such as “*Outdoor Bike recorded between minute 1121 and 1133*”. We use 20 rewrite templates in total for semantic captions.

A.3. Downstream Datasets

Table 7 summarizes the demographic distributions for the downstream linear probing and few-shot evaluation datasets: the *Activity dataset* and the *Metabolic dataset*. For zero-shot classification tasks, we resample the test data to create a more balanced evaluation set. Additional details, including the number of samples per class, are provided in Appendix B.5.

Table 6 | **Definitions of sensor features.** We detail the names, units, and definitions of the 26 features derived from PPG, accelerometer, skin conductance, skin temperature, and altitude signals.

Feature	Unit	Definition
Photoplethysmography (PPG)		
Heart Rate	Beats/Min	Mean of instantaneous heart rate.
Shannon Ent. RR	Nats	Shannon entropy of the RR intervals.
Shannon Ent. RR Diffs	Nats	Shannon entropy of the RR interval differences.
RMSSD	Msec	Root mean squared st. dev. of RR intervals.
SDNN	Msec	Standard deviation of RR intervals.
RR Percent Valid	%	% of 5-minute window with valid RR intervals.
RR 80 th Percentile	Msec	80 th percentile of 5-minute window of RR intervals.
RR 20 th Percentile	Msec	20 th percentile of RR intervals.
RR Median	Msec	Median RR interval.
Heart Rate at Rest	Beats/Min	Mean of heart rate at rest.
Accelerometer (ACC)		
Step Count	Steps	Number of steps.
Jerk Autocorrelation Ratio	a.u.	Ratio of lag=1 autocorrelation to energy in 1st 3-axis principal component.
Log Energy	a.u.	Log of sum of 3-axis root mean squared magnitude.
Covariance Condition	a.u.	Estimate of condition number for 3-axis covariance matrix.
Log Energy Ratio	a.u.	Log of ratio of sum of energy in 1st 3-axis principal component over energy of 3-axis root mean squared magnitude.
Zero Crossing St.Dev.	Seconds	Standard deviation of time between zero crossing of 1st 3-axis principal component.
Zero Crossing Average	Seconds	Mean of time between zero crossing of 1st 3-axis principal component.
Axis Mean	a.u.	Mean of 3-axis.
Kurtosis	a.u.	Kurtosis of 3-axis root mean squared magnitude.
Sleep Coefficient	a.u.	Sum of 3-axis max-min range, binned into 16 log-scaled bins.
Skin Conductance (EDA)		
Skin Conductance Value	μ Siemens	Center of linear tonic SCL value fit.
Skin Conductance Slope	μ S/Min	Intraminute slope of SCL values.
Lead Contact Counts	Counts	Number of times leads of the sensor contacting wrist in a minute.
Skin Temperature (TEMP)		
Skin Temperature Value	°C	Value of skin temperature.
Skin Temperature Slope	°C/Min	Slope of skin temperature.
Altimeter (ALT)		
Altitude St.Dev. Norm	Hectopascals	Standard deviation of altimeter readings.

Table 7 | Detailed statistics and demographic information for the pretraining and downstream datasets. We report participant counts for the pretraining, *Activity* (downstream), and *Metabolic* (downstream) datasets, along with demographic breakdowns by sex, age, and BMI.

Category	Pretraining	Activity (downstream)		Metabolic (downstream)	
		train	test	train	test
Sex:					
Male	64,194	27,653	6,092	551	258
Female	39,376	10,145	2,248	670	455
Not Specified	73	24	3	0	0
Age:					
18 – 39	52,004	19,340	4,492	415	223
40 – 59	41,296	15,309	3,172	637	384
60 – 79	9,340	2,875	618	198	121
≥ 80	676	120	31	0	1
Not Specified	327	30	0	0	0
BMI:					
Healthy (< 25)	38,582	15,942	3,685	319	188
Overweight (25 – 30)	34,188	14,154	3,017	343	206
Obese (≥ 30)	25,969	6,131	1,316	481	274
Not Specified	324	81	18	49	28
Total	103,643	37,822	8,343	1,250	729

Table 8 | Example of prompt templates used in statistical captions.

Statistical Caption Templates
<ol style="list-style-type: none"> 1. The average Heart rate value is 88.7, with extremes at 134.9 (max) and 70.8 (min), and a std of 9.3. 2. The Heart rate data exhibits a mean of 88.7, a standard deviation of 9.3, and its extreme values are 70.8 and 134.9. 3. Heart rate average 88.7, reaching a maximum of 134.9 and a minimum of 70.8, with a standard deviation of 9.3. 4. Heart rate exhibits a mean of 88.7, with peak and minimal values reaching 134.9 and 70.8, and a standard deviation of 9.3. 5. For the Heart rate measurements, the mean is 88.7, the standard deviation is 9.3, and the data lies between 70.8 and 134.9.

A.4. Data Acquisition and Approval

The data used for training in our analysis was curated from a large corpus of historical wearable data collected with consent from participants for these data to be used in research. Specifically, the

Table 9 | Example of prompt templates used in structural captions.

Structural Caption Templates
Trends:
1. An decreasing trend in Heart rate data recorded between minute 680 and 960.
2. Heart rate exhibits decreasing trend during minute 680-960 interval.
3. An decreasing trend in Heart rate data recorded between minute 680 and 960.
4. The Heart rate trend from minute 680 to 960 is decreasing.
5. From minute 680 to 960, Heart rate exhibits an decreasing trend.
.....
Spikes:
1. Spike event recorded for steps at minute 720.
2. Data indicates a peak for steps at the 720-minute mark.
3. Minute 720 shows a spike for the steps.
4. A peak is detected for steps at minute 720.
5. The steps experienced a spike at minute 720.
.....

Table 10 | Example of prompt templates used in semantic captions.

Semantic Caption Templates
1. From minute 1121 to 1133, the user had a period of Outdoor Bike.
2. Outdoor Bike recorded within the 1121-1133 minute range.
3. Outdoor Bike episode occurred between minute 1121 and 1133.
4. Outdoor Bike was recorded between minute 1121 and 1133.
5. Identified Outdoor Bike across the timeframe of minute 1121 to 1133.
.....

consent language described use of the data for developing new health features and algorithms and being included in publications: “*Fitbit will collect and use your data to research and develop new health and wellness products and services for you and others. This data includes your: Health and wellness data, such as steps, heart rate, and sleep data. Your data may also be used to generate findings that could be included in publications (such as scientific journals) to contribute to general knowledge about health and science. For example, activity, heart rate, and sleep data contributed to published findings that Fitbit devices could help detect flu outbreaks. None of the data used for these purposes will include your name, email, or other information that directly identifies you.*”

The use of data for pretraining in this manner was approved as exempt under 45 CFR § 46.104(d)(4) “because the research involves the use of identifiable private information/biospecimens; and information, which may include information about biospecimens, is recorded by the investigator in such a manner that

Table 11 | **The SensorLM family.** SensorLM consists of four variants with increasing model sizes. Architectural details for the sensor encoder, text encoder, and multimodal text decoder are provided.

Model	Sensor Encoder			Text Encoder & Multimodal Decoder				Sensor / Text	
	layers	MLP	# params	layers _{enc}	layers _{dec}	MLP	# params	hidden	heads
SensorLM-S	12	512	3M	12	3	512	12M	128	16
SensorLM-B	12	3072	114M	12	3	3072	191M	768	12
SensorLM-L	24	4096	404M	24	3	4096	519M	1024	16
SensorLM-XL	40	5632	1.27B	40	3	5632	1.45B	1408	16

the identity of the human subjects cannot readily be ascertained directly or through identifiers linked to the subjects, the investigator does not contact the subjects, and the investigator will not re-identify subjects.”

The Metabolic downstream dataset for anxiety, hypertension prediction came from an IRB approved study (protocol number Pro00074093). The core objective of this study as described in the IRB protocol was to: “Evaluate the feasibility of using the data provided by wrist-worn wearable devices to develop algorithms and scores to assess metabolic health.”

In the consent for the observational study, participants were informed that data on up to 7,500 participants in the United States would be collected. We used a mobile study platform that allows participants to enroll, check eligibility and provide full informed consent. The same mobile application enables the collection of Fitbit data using Fitbit devices or Pixel watches and allows participants to complete questionnaires. The participants reported their anxiety, depression and hypertension diagnoses through this app. Data was de-identified and stored in accordance with the approved IRB protocol. The participants were compensated with a free set of lab tests from Quest Diagnostics for participating in the study.

B. Implementation Details

B.1. SensorLM Model Architecture

As described earlier, SensorLM consists of a sensor encoder, a text encoder, and a multimodal text decoder (Fig. 3). The input to the sensor encoder is a matrix of shape [26 features × 1440 minutes], representing one-day windows of sensor data at minutely resolution. The sensor encoder is built using a ViT-2D backbone with a 2D patch size of (2, 10), producing 1872 tokens.

The text encoder and multimodal text decoder follow standard transformer architectures. The multimodal text decoder attends to the output tokens of the sensor encoder via cross-attention [38], enabling an encoder-decoder setup for caption generation. For contrastive learning, we use representations from the sensor encoder and unimodal text encoder. Both representations are average-pooled, passed through projection heads, normalized, and then used to compute the contrastive loss \mathcal{L}_{con} between sensor embeddings s_i and text embeddings v_i .

The SensorLM family consists of four variants with different (increasing) model sizes: SensorLM-S, SensorLM-B, SensorLM-L, and SensorLM-XL. Architectural specifications for each variant are provided in Table 11.

Table 12 | Hyperparameters for self-supervised learning baselines. We provide settings used for MSN [2], DINO [3], and SimCLR [5]. A single row value indicates that the setting was applied to all methods.

Configuration	MSN [2]	DINO [3]	SimCLR [5]
training steps		50,000	
warmup steps		2,500	
optimizer		AdamW [18]	
opt. momentum $[\beta_1, \beta_2]$		[0.9, 0.99]	
base learning rate	0.001	0.004	0.001
batch size		1,024	
weight decay		0.0001	
gradient clipping		3.0	
learning rate schedule		linear warmup & cosine decay	
data resolution		26 (sensor) \times 1440 (minutes)	

B.2. Pretraining Details

All models are trained using the SensorLM pretraining objective ($\mathcal{L}_{\text{SensorLM}}$) on Google v6 TPUs for 50k steps. We use a batch size of 1024 sensor-text pairs, with $\lambda_{\text{con}} = \lambda_{\text{cap}} = 1$ for main experiments. The temperature τ for the contrastive loss is set to 0.01. Optimization is performed using Adam optimizer with $\beta_1 = 0.9$ and $\beta_2 = 0.95$. A cosine warm-up schedule is applied for the first 10% of training steps, followed by linear decay of the learning rate to zero.

Appendix C.1 provides compute and training time details for different model variants and data sizes in the context of scaling analysis for SensorLM.

B.3. Self-Supervised Learning Baselines

We compare SensorLM against the following self-supervised learning (SSL) baselines:

- **SimCLR [5]** is a widely adopted contrastive learning framework that aligns representations from augmented views of the same input while repelling those of different inputs. It relies solely on contrastive loss and unlabeled data, and has proven effective for both visual and text-based representation learning.
- **MSN [2]** integrates contrastive-based pretraining with masked image modeling. MSN aligns the representation of a masked view with that of the unmasked input by processing only visible patches. This approach enhances scalability with Vision Transformers and yields semantically meaningful features, achieving strong performance in low-shot classification tasks.
- **DINO [3]** employs a self-distillation strategy using a teacher-student framework. The student network is trained to match the teacher’s representations across different augmentations. DINO has demonstrated robust and generalizable feature learning across various domains.

All three baselines follow augmentation-driven training paradigms. We apply a standardized set of time-series augmentations (e.g., jittering, scaling, time flipping) based on prior work [17, 26, 27, 41]. Each augmentation is applied independently with a probability of 0.5. Jittering adds Gaussian noise with zero mean and a standard deviation uniformly sampled from [0, 0.5]. Scaling multiplies the input by a random factor sampled from [1.1, 1.5]. Notably, we omit scaling for DINO

Table 13 | Definition of the activity-related concept classification tasks.

Class	Activities included	Prompt example
Task: Environmental context		
Indoor Sports	Elliptical, Treadmill, Spinning, Weightlifting, Yoga, Core training, Pilates, Stairclimber, Dancing, Indoor climbing, Kickboxing	User performed Indoor Sports.
Outdoor Sports	Bike, Run, Hike, Tennis, Mountain Bike, Rollerblading, Golf	User performed Outdoor Sports.
Water Sports	Swim, Kayaking, Surfing, Paddleboarding	User performed Water Sports.
Winter Sports	Skiing, Snowboarding	User performed Winter Sports.
Task: Locomotion vs. stationary		
Locomotion Exercise	Walk, Run, Hike, Stairclimber, Treadmill, Elliptical	User performed Locomotion exercise.
Stationary Exercise	Weightlifting, Yoga, Core training, Pilates	User performed Stationary exercise.
Task: Cardio vs. strength training		
Cardio Exercise	Elliptical, Treadmill, Spinning, Stairclimber, Run	User performed Cardio exercise.
Strength Exercise	Weightlifting, Core training, Indoor climbing	User performed Strength exercise.

due to convergence issues observed during training.

All baseline models are pretrained from scratch under training settings listed in Table 12. For consistency, all methods use the same ViT-2D backbone as the sensor encoder in SensorLM, with a 2D patch size of (2, 10).

B.4. LLM Baselines

For zero-shot classification, cross-modal retrieval, and sensor captioning, we compare SensorLM against two LLMs: Gemini 2.0 Flash [28] and Gemma-3-27B [29], by formatting sensor data as tabular input.

- **Gemma-3-27B [29]** is a state-of-the-art open-weight large language model developed by Google DeepMind. Trained on a high-quality, multilingual corpus, it is optimized for instruction following and reasoning tasks. We use the instruction-tuned variant, which exhibits strong performance in both zero-shot and few-shot scenarios.
- **Gemini 2.0 Flash [28]** is a lightweight, high-performance member of Google’s Gemini multimodal model family, designed for latency-sensitive applications. It supports vision-language reasoning and offers strong cross-modal capabilities with low inference latency.

For both baselines, we subsample the sensor data to fit within the context length limitations of these LLMs.

Table 14 | Example of templates used in zero-shot prompt ensemble.

Zero-Shot Templates
1. A period of Run was observed during the session. 2. Detected a phase of Run. 3. Data shows Run took place 4. The main action was Run 5. Run was detected during the observed period.

B.5. Zero-Shot Classification

B.5.1. Task definition for zero-shot classification

We formulate six zero-shot classification tasks related to activity recognition. We compare SensorLM with representative LLM baselines across *main activity classification*, *activity-related concept classification*, and *fine-grained recognition*, aiming to evaluate the effectiveness of SensorLM in diverse human activity analysis scenarios.

Main activity classification encompasses 20 activities. For each activity, the number of samples is indicated in parentheses. These include: *Walking* (881), *Bike* (860), *Playing Sports* (905), *Running* (793), *Aerobics* (910), *Elliptical* (887), *Spinning* (866), *Weightlifting* (842), *Swimming* (882), *Hiking* (848), *Playing Tennis* (821), *CrossFit* (902), *Pilates* (855), *Stairclimber* (863), *Dancing* (852), *Indoor climbing* (854), *Golf* (710), *Skiing* (420), *Snowboarding* (167), and *Kayaking* (212).

For **activity-related concept classification**, we define three sub-tasks. The first one, “*Activity by environmental context*”, comprises four classes: *Indoor Sports*, *Outdoor Sports*, *Water Sports*, and *Winter Sports*. The second task, “*Cardio vs. strength training*”, distinguishes between two classes: *Cardio exercise* and *Strength exercise*. Similarly, for the third task, “*Locomotion vs. stationary*”, we have two classes: *Locomotion exercise* and *Stationary exercise*. The activities included in each concept category are summarized in Table 13.

Finally, we introduce two **fine-grained recognition** tasks. The first task, “*Fine-grained recognition (Gym cardio)*”, differentiates among *Elliptical* (887), *Treadmill* (884), *Spinning* (866), and *Stairclimber* (863). The second task, “*Fine-grained recognition (outdoor sports)*”, involves classifying among *Hike* (848), *Mountain Bike* (673), *Skiing* (420), and *Snowboarding* (167).

B.5.2. Implementation for zero-shot classification

Implementation details for SensorLM. We employ prompt ensembling [24] using a diverse set of rewritten prompts that mirror the structure of pretraining captions. For each label class, we compute the average embedding from the text encoder across all prompts. Zero-shot classification is performed by selecting the label whose average text embedding is most similar to the sensor embedding from the sensor encoder. Examples of the prompts are provided in Table 14; we use a total of 30 prompts.

Implementation details for LLM baselines. For zero-shot classification using LLM baselines (i.e., Gemini 2.0 Flash [28] and Gemma-3-27B [29]), we employ a prompt format illustrated in Table 15. The prompt instructs the model to predict a class label based on the provided sensor data, which is formatted as tabular input.

Table 15 | Zero-shot classification prompt used for LLM baselines.

Zero-Shot Classification Prompt

```

### Overall instruction: Your job is to identify user activity class by analyzing a given day of Fitbit data.
Available Activity Classes: {class_list}

### Sensor Description
##### Heart:
HR: Mean of the instantaneous heart rate in beats per minute. Calculated over a 1 minute window. Unit: Beats/Min
hr_at_rest_mean: Mean of the heart rate in beats per minute during periods of rest. Unit: Beats/Min
hrv_rr_80th_percentile_mean: The 80th percentile of the RR intervals in milliseconds for 5-minute windows with valid RR intervals. Unit: Msec
hrv_rr_20th_percentile_mean: The 20th percentile of the RR intervals in milliseconds for 5-minute windows with valid RR intervals. Unit: Msec
hrv_rr_median: The median RR interval in milliseconds for 5-minute windows with valid RR intervals. Unit: Msec
hrv_shannon_entropy_rr: Shannon entropy of the RR intervals for 5-minute windows with valid RR intervals. Unit: Nats
hrv_shannon_entropy_rrd: Shannon entropy of the RR interval differences for 5-minute windows with valid RR intervals. Unit: Nats
rmssd_percentile_0595: Root mean squared standard deviation of RR intervals in milliseconds for 5-minute windows with valid RR intervals. Unit: Msec
sdnn_percentile_0595: Standard deviation of RR intervals in milliseconds for 5-minute windows with valid RR intervals. Unit: Msec
#####
Activity:
steps: Number of steps calculated over a 1 minute window. Unit: Steps
jerk_auto: Ratio of lag=1 autocorrelation to energy in 1st 3-axis principal component. Unit: alog_energy
log_energy: Log of sum of 3-axis root mean squared magnitude. Unit: alog_energy
covariance: Estimate of condition number for 3-axis covariance matrix. Unit: acovariance
log_energy_ratio: Log of ratio of sum of energy in 1st 3-axis principal component over energy of 3-axis root mean squared magnitude. Unit: alog_energy_ratio
zero_crossing_std: Standard deviation of time between zero crossings of 1st 3-axis principal component. Unit: Seconds
zero_crossing_avg: Mean of the time between zero crossings of 1st 3-axis principal component in seconds. Unit: Seconds
axis_mean: Log of the mean square root of the squared X & Z axes of the accelerometer. Unit: a.u.
altim_std: Standard deviation of altimeter readings in Hectopascals. Unit: Hectopascals
kurtosis: Kurtosis of the 3-axis accelerometer root mean squared magnitude. Unit: a.u.
#####
Sleep:
sleep_coefficient: Sum of 3-axis max-min range, binned into 16 log-scaled bins. Unit: aSleep
#####
EDA:
eda_level_real: Mean tonic skin conductance value in micro Siemens over a 1 minute window. Unit:  $\mu$ Siemens
leads_contact_counts: Number of times the skin conductance sensor electrode leads make contact (likely related to signal quality). Unit: Counts
ceda_slope_real_micro_siemens: Intraminate slope of SCL values. Unit:  $\mu$ Siemens/Min
skin_temperature_slope: Change in skin temperature in degrees Celsius per minute over a 1 minute window. Unit: °C/Min
wrist_temperatures: Mean skin temperature in degrees Celsius calculated over a 1 minute window. Unit: °C
#### Here is an example output with the predicted activity class and reasoning behind the choice:
{{
    "predicted_class": <predicted_class>,
    "class_probabilities": {{{
        "class 1": <probability_of_class_1>,
        "class 2": <probability_of_class_2>,
        "class 3": <probability_of_class_3>,
        "class 4": <probability_of_class_4>,
        ....
        ....
    }}},
    "reasoning": <reasoning>
}}
#### Now, it is your turn. Here is a day of Fitbit data for a user in csv format. Each row is a window of 10-minute average values for the corresponding feature metric. Analyse the Fitbit data thoroughly and make the prediction.
{sensor_data}
### Your output in JSON format containing the predicted class and class probabilities for all classes. The class probabilities should sum to 1. The predicted class should be from Available Activity Classes list mentioned earlier. No other classes apart from them should be used. Also give a reason for your prediction.

```

Table 16 | Zero-shot cross-modal retrieval prompt used for LLM baselines.

Zero-Shot Cross-Modal Retrieval Prompt

```

### Overall instruction: You will be given a day of user Fitbit data and a set of 100 captions. Your job is to
analyze the Fitbit data and select top 10 captions that describe the Fitbit data the best.

#### Sensor Description

##### Heart:
HR: Mean of the instantaneous heart rate in beats per minute. Calculated over a 1 minute window. Unit: Beats/Min
hr_at_rest_mean: Mean of the heart rate in beats per minute during periods of rest. Unit: Beats/Min
hrv_rr_80th_percentile_mean: The 80th percentile of the RR intervals in milliseconds for 5-minute windows with valid
RR intervals. Unit: Msec
hrv_rr_20th_percentile_mean: The 20th percentile of the RR intervals in milliseconds for 5-minute windows with valid
RR intervals. Unit: Msec
hrv_rr_median: The median RR interval in milliseconds for 5-minute windows with valid RR intervals. Unit: Msec
hrv_shannon_entropy_rr: Shannon entropy of the RR intervals for 5-minute windows with valid RR intervals. Unit: Nats
hrv_shannon_entropy_rrd: Shannon entropy of the RR interval differences for 5-minute windows with valid RR
intervals. Unit: Nats
rmssd_percentile_0595: Root mean squared standard deviation of RR intervals in milliseconds for 5-minute windows with
valid RR intervals. Unit: Msec
sdnn_percentile_0595: Standard deviation of RR intervals in milliseconds for 5-minute windows with valid RR
intervals. Unit: Msec

##### Activity:
steps: Number of steps calculated over a 1 minute window. Unit: Steps
jerk_auto: Ratio of lag=1 autocorrelation to energy in 1st 3-axis principal component. Unit: alog_energy
log_energy: Log of sum of 3-axis root mean squared magnitude. Unit: alog_energy
covariance: Estimate of condition number for 3-axis covariance matrix. Unit: acovariance
log_energy_ratio: Log of ratio of sum of energy in 1st 3-axis principal component over energy of 3-axis root mean
squared magnitude. Unit: alog_energy_ratio
zero_crossing_std: Standard deviation of time between zero crossings of 1st 3-axis principal component. Unit: Seconds
zero_crossing_avg: Mean of the time between zero crossings of 1st 3-axis principal component in seconds. Unit: Seconds
axis_mean: Log of the mean square root of the squared X & Z axes of the accelerometer. Unit: a.u.
altim_std: Standard deviation of altimeter readings in Hectopascals. Unit: Hectopascals
kurtosis: Kurtosis of the 3-axis accelerometer root mean squared magnitude. Unit: a.u.

##### Sleep:
sleep_coefficient: Sum of 3-axis max-min range, binned into 16 log-scaled bins. Unit: aSleep

#### EDA:
eda_level_real: Mean tonic skin conductance value in micro Siemens over a 1 minute window. Unit:  $\mu$ Siemens
leads_contact_counts: Number of times the skin conductance sensor electrode leads make contact (likely related to
signal quality). Unit: Counts
ceda_slope_real_micro_siemens: Intraminate slope of SCL values. Unit:  $\mu$ Siemens/Min
skin_temperature_slope: Change in skin temperature in degrees Celsius per minute over a 1 minute window. Unit: °C/Min
wrist_temperatures: Mean skin temperature in degrees Celsius calculated over a 1 minute window. Unit: °C

### Here is an example output structure with the predicted top 10 captions:
{
  "first": <caption_ID>,
  "second": <caption_ID>,
  "third": <caption_ID>,
  "fourth": <caption_ID>,
  "fifth": <caption_ID>,
  "sixth": <caption_ID>,
  "seventh": <caption_ID>,
  "eighth": <caption_ID>,
  "ninth": <caption_ID>,
  "tenth": <caption_ID>
}

### Now, it is your turn. Here is a day of Fitbit data for a user in csv format. Each row is a window of 10-minute
average values for the corresponding feature metric. Analyze the Fitbit data thoroughly and choose
top 10 captions from the list which best describe the Fitbit data.
{sensor_data}

Here is the set of 100 captions:
{caption_list}

### Your output in JSON format containing the predicted top 10 caption ids:

```

Table 17 | Caption generation prompt used for LLM baselines.

Caption Generation Prompt
<pre>### Overall instruction: You will be given a day of user Fitbit data. Your job is to analyze the Fitbit data and generate a caption containing semantic information. Semantic information aims to capture the high-level meaning and context embedded in the sensor data, essentially interpreting what the individual might be doing or experiencing. ### Sensor Description ##### Heart: HR: Mean of the instantaneous heart rate in beats per minute. Calculated over a 1 minute window. Unit: Beats/Min hr_at_rest_mean: Mean of the heart rate in beats per minute during periods of rest. Unit: Beats/Min hrv_rr_80th_percentile_mean: The 80th percentile of the RR intervals in milliseconds for 5-minute windows with valid RR intervals. Unit: Msec hrv_rr_20th_percentile_mean: The 20th percentile of the RR intervals in milliseconds for 5-minute windows with valid RR intervals. Unit: Msec hrv_rr_median: The median RR interval in milliseconds for 5-minute windows with valid RR intervals. Unit: Msec hrv_shannon_entropy_rr: Shannon entropy of the RR intervals for 5-minute windows with valid RR intervals. Unit: Nats hrv_shannon_entropy_rrd: Shannon entropy of the RR interval differences for 5-minute windows with valid RR intervals. Unit: Nats rmsd_percentile_0595: Root mean squared standard deviation of RR intervals in milliseconds for 5-minute windows with valid RR intervals. Unit: Msec sdm_percentile_0595: Standard deviation of RR intervals in milliseconds for 5-minute windows with valid RR intervals. Unit: Msec ##### Activity: steps: Number of steps calculated over a 1 minute window. Unit: Steps jerk_auto: Ratio of lag=1 autocorrelation to energy in 1st 3-axis principal component. Unit: alog_energy log_energy: Log of sum of 3-axis root mean squared magnitude. Unit: alog_energy covariance: Estimate of condition number for 3-axis covariance matrix. Unit: acovariance log_energy_ratio: Log of ratio of sum of energy in 1st 3-axis principal component over energy of 3-axis root mean squared magnitude. Unit: alog_energy_ratio zero_crossing_std: Standard deviation of time between zero crossings of 1st 3-axis principal component. Unit: Seconds zero_crossing_avg: Mean of the time between zero crossings of 1st 3-axis principal component in seconds. Unit: Seconds axis_mean: Log of the mean square root of the squared X & Z axes of the accelerometer. Unit: a.u. altim_std: Standard deviation of altimeter readings in Hectopascals. Unit: Hectopascals kurtosis: Kurtosis of the 3-axis accelerometer root mean squared magnitude. Unit: a.u. ##### Sleep: sleep_coefficient: Sum of 3-axis max-min range, binned into 16 log-scaled bins. Unit: aSleep ##### EDA: eda_level_real: Mean tonic skin conductance value in micro Siemens over a 1 minute window. Unit: μSiemens leads_contact_counts: Number of times the skin conductance sensor electrode leads make contact (likely related to signal quality). Unit: Counts ceda_slope_real_micro_siemens: Intraminate slope of SCL values. Unit: μSiemens/Min skin_temperature_slope: Change in skin temperature in degrees Celsius per minute over a 1 minute window. Unit: °C/Min wrist_temperatures: Mean skin temperature in degrees Celsius calculated over a 1 minute window. Unit: °C ##### Here are some example captions: Example 1: Period of Outdoor Bike noted from minute 912 until 917. Outdoor Bike occurred from minute 619 to 628. Outdoor Bike recorded within the 641-650 minute range. User engaged in Outdoor Bike between minute 928 and 937. Outdoor Bike took place during the minutes 492 through 502. User engaged in Outdoor Bike between minute 720 and 730. From minute 446 to 456, the user had a period of Outdoor Bike. Outdoor Bike took place during the minutes 572 through 584. Example 2: Observed Walk spanning minutes 402 to 408. An instance of Walk was identified from minute 652 to 663. A continuous Walk phase from minute 692 to 703. Detection of Walk activity between minute 1021 and 1035. A Walk period between minutes 651 and 668. Walk was recorded between minute 785 and 822. A Sleep period between minutes 1346 and 1440. Example 3: An instance of Walk was identified from minute 279 to 289. An instance of Walk was identified from minute 799 to 828. A Walk period between minutes 279 and 309. Sleep occurred from minute 1303 to 1440. Example 4: Walk state observed from minute 1132 up to 1139. Outdoor Bike between minutes 1051 and 1064. Outdoor Bike state observed from minute 489 up to 505. Sleep occurred from minute 4 to 400. The person logged their mood as Excited at minute 1204. The person registered a mood of Frustrated at minute 773. At minute 773, the individual's feeling is Frustrated. ### Now, it is your turn. Here is a day of Fitbit data for a user in csv format. Each row is a window of 10-minute average values for the corresponding feature metric. Analyse the Fitbit data thoroughly and generate the caption which best describe the Fitbit data. {sensor_data} ### Your output:</pre>

B.6. Few-Shot Learning

For both few-shot learning and linear probing tasks, the sensor encoder of SensorLM is frozen. A single linear layer¹ is trained using a multinomial loss with balanced class weights (weights inversely proportional to class frequencies in the training set). This same approach is applied to all SSL baselines for consistency.

For linear probing, we use the full training set (statistics provided in Table 7). For few-shot learning, we randomly sample 5–50 training examples per class and repeat each experiment five times with different random seeds. Table 18 summarizes the class distribution for the “Anxiety” and “Hypertension” tasks.

B.7. Cross-Modal Retrieval

Implementation details for SensorLM. To evaluate zero-shot cross-modal retrieval, we use top- k recall ($R@k$) for $k \in \{1, 5, 10\}$. This metric measures the proportion of queries for which the ground-truth pairing appears within the top k retrieved results. Retrieval is conducted in both Sensor → Text and Text → Sensor directions. Cosine similarity between sensor and text embeddings is used as the scoring function to rank candidates. For each query, recall is computed by locating the ground-truth index within the ranked similarity list.

Implementation details for LLM baselines. For zero-shot cross-modal retrieval using the LLM baselines (i.e., Gemini 2.0 Flash [28] and Gemma-3-27B [29]), we use a prompt format illustrated in Table 16. The prompt instructs the model to retrieve the top-10 most relevant captions from a set of 100 candidates, based on the provided sensor data formatted as tabular input. We evaluate only in the Sensor → Text direction, as Text → Sensor retrieval is not feasible due to the context length limitations of the LLMs.

B.8. Zero-Shot Generalization to Unseen Classes

To assess SensorLM’s generalization to novel activities, we conduct a case study involving pretraining on a dataset comprising data only containing 20 activities, followed by testing exclusively on a set of 9 previously unseen classes.

The 20 activities used in the pretraining set include: *Bike, Playing Sports, Running, Aerobics, Elliptical, Weightlifting, Swimming, Hiking, Playing Tennis, CrossFit, Core training, Pilates, Bootcamp, Indoor Climbing, Golf, Kickboxing, Skiing, Rollerblading, and Kayaking*.

The 9 unseen activities evaluated are: *Snowboarding* (167), *Mountain Bike* (673), *Racquetball* (19), *Yoga* (879), *Paddleboarding* (51), *Badminton* (109), *Dancing* (852), *Calisthenics* (61) and *Basketball* (127).

For each unseen activity, we evaluate SensorLM’s zero-shot performance using a one-versus-all classification setup. The primary evaluation metric is the Area Under the Receiver Operating Characteristic Curve (AUROC), with 95% bootstrap confidence intervals (CIs) computed using 1000 resampling iterations with replacement [4].

¹https://scikit-learn.org/stable/modules/generated/sklearn.linear_model.LogisticRegression.html

Table 18 | Class distribution for the Anxiety and Hypertension prediction tasks.

Task / Label	Train	Test
Anxiety		
positive	55,030	34,749
negative	96,316	55,437
Hypertension		
positive	36,349	23,353
negative	114,997	66,833
Total		
	151,346	90,186

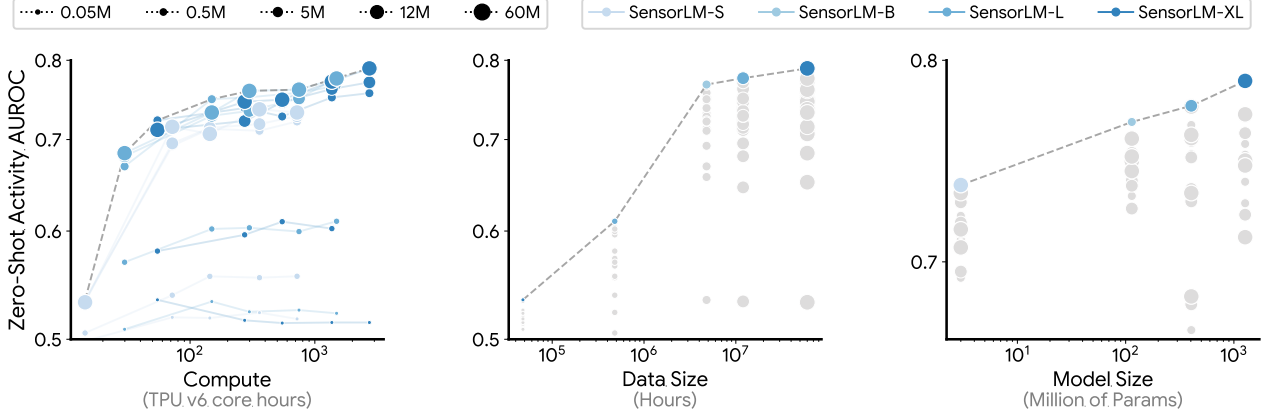


Figure 8 | **Scaling behaviors of SensorLM.** We show the zero-shot downstream performance of SensorLM as a function of compute (left), data size (middle), and model size (right). Results demonstrate that increasing compute, data, and model size each leads to consistent performance gains.

B.9. Caption Generation

Implementation details for SensorLM. For sensor captioning, we observe that increasing the number of layers in the multimodal text decoder improves captioning performance. Accordingly, we train a SensorLM-B model with 12 decoder layers (compared to the default 3) using *semantic captions* during pretraining. During inference, captions are generated autoregressively from sensor data using a [START] token.

Implementation details for LLM baselines. For caption generation using LLM baselines (i.e., Gemini 2.0 Flash [28] and Gemma-3-27B [29]), we use prompt templates shown in Table 17. These prompts instruct the model to generate a semantic caption based on the provided sensor data, formatted as tabular input.

C. Additional Results

C.1. Scaling Behaviors

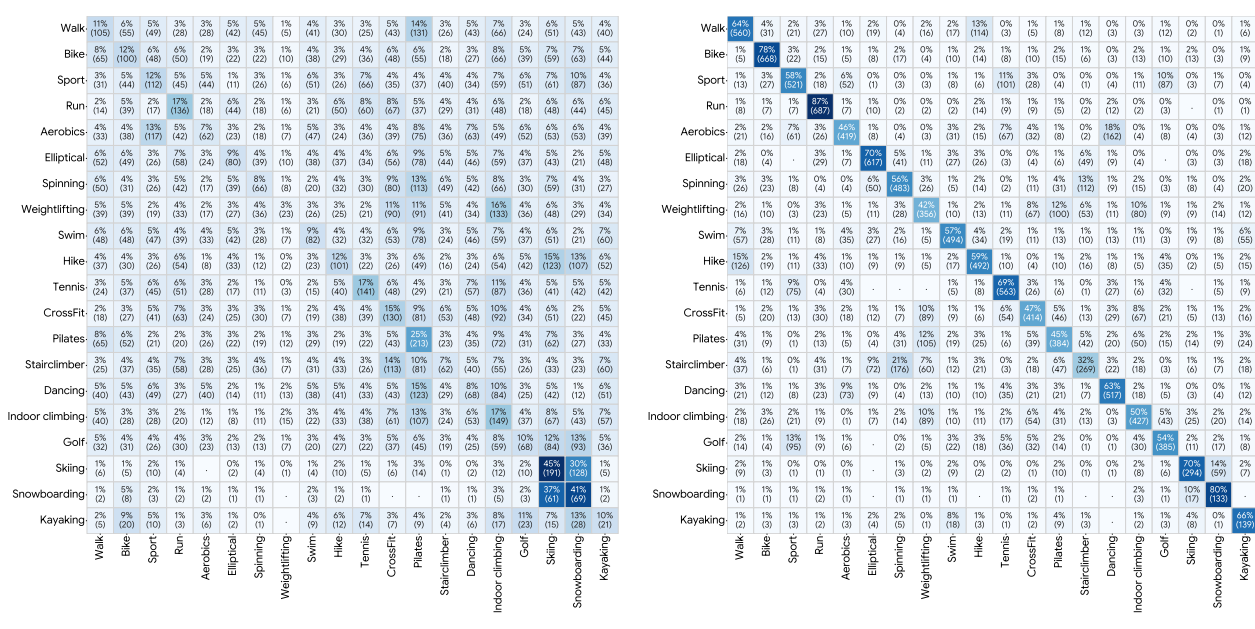
We investigate the scaling behaviors in SensorLM when trained on large-scale wearable data and captions, analyzing how compute (training steps), data size, and model size influence performance on zero-shot activity recognition. Fig. 8 presents the Pareto front of AUROC scores.

Compute scaling: Increasing training steps from 1k to 10k consistently improves downstream performance; for instance, SensorLM-B improves from an AUROC of 0.66 at 17.4 TPU hours to 0.75 at 174 TPU hours.

Data scaling: Expanding training data yields consistent gains, especially for larger models. However, gains beyond 12 million hours diminish, showing saturation trends as reported in prior work [12].

Model scaling: Larger models like SensorLM-XL and SensorLM-L outperform smaller counterparts given sufficient compute and data. At low training steps, SensorLM-XL underperforms due to undertraining, a phenomenon consistent with scaling law observations.

Overall, SensorLM demonstrates consistent and predictable scaling behaviors, highlighting the applicability of scaling laws to sensor-language modeling and motivating future work on scaling model capacity and data volume.



(a) SimCLR [5]

(b) SensorLM

Figure 9 | Confusion matrices for linear probing activity classification. Comparison of SimCLR [5] and SensorLM-trained sensor encoders on the downstream Activity dataset for 20-class classification. The y-axis represents ground truth labels, and the x-axis shows predicted labels.

Table 19 | **Linear probing results.** We use all data for task-specific linear probing. AUROC[†] is used as the metric. Best results of each column are in **bold** and the second best are underlined.

Task	Hypertension	Anxiety	Activity
SimCLR [5]	0.56	0.64	0.68
DINO [3]	0.56	0.62	0.66
MSN [2]	<u>0.58</u>	0.66	<u>0.72</u>
SensorLM	0.60	<u>0.65</u>	0.94

C.2. Few-Shot Learning & Linear Probing

Table 19 presents task-specific linear probing results for SensorLM compared to several SSL baselines: SimCLR, DINO, and MSN. All evaluations use the full available training data, and performance is measured by AUROC. SensorLM achieves competitive or superior performance across all tasks, with the highest AUROC for “*Hypertension*” (0.60) and “*Activity*” (0.94). For “*Anxiety*”, SensorLM (0.65) performs comparably to MSN (0.66), the top-performing baseline for that task. These results highlight SensorLM’s robust representation learning for downstream applications.

Fig. 9 shows confusion matrices for SensorLM and SimCLR, illustrating the improved discriminative capability of SensorLM embeddings across diverse activity classes.

We also include results on two regression tasks: predicting Age and BMI from one day of sensor data. Using a frozen sensor encoder and a linear regression probe², we report Mean Absolute Error

²https://scikit-learn.org/stable/modules/generated/sklearn.linear_model.LinearRegression.html

Table 20 | Performance of SensorLM and baselines on regression tasks.

Metrics	Age		BMI	
	MAE \downarrow	MAPE \downarrow	MAE \downarrow	MAPE \downarrow
SimCLR	9.18	21.03	5.85	19.57
DINO	9.63	22.03	5.97	19.97
MSN	9.36	21.39	5.84	19.53
SensorLM	9.18	20.81	5.75	19.17

Table 21 | Zero-shot cross-modal retrieval. We evaluate cross-modal retrieval on a held-out dataset containing 40,000 examples, testing performance across varying retrieval set sizes. SensorLM achieves consistently strong retrieval performance across all settings. For baseline LLMs, most retrieval tasks are infeasible due to context length limitations (marked as “–”).

Metrics	100 samples			5,000 samples			40,000 samples		
	R@1	R@5	R@10	R@1	R@5	R@10	R@1	R@5	R@10
<i>Sensor → Text:</i>									
Gemma-3-27B [29]	1.0	5.0	10.0	–	–	–	–	–	–
Gemini 2.0 [28]	5.0	9.0	13.0	–	–	–	–	–	–
SensorLM	100.0	100.0	100.0	98.2	99.4	99.6	96.1	98.7	99.0
<i>Text → Sensor:</i>									
Gemma-3-27B [29]	–	–	–	–	–	–	–	–	–
Gemini 2.0 [28]	–	–	–	–	–	–	–	–	–
SensorLM	100.0	100.0	100.0	96.7	99.2	99.4	90.0	96.9	98.1

(MAE) and Mean Absolute Percentage Error (MAPE). As shown in Table 20, SensorLM improves performance compared to SSL baselines.

C.3. Cross-Modal Retrieval

Table 21 presents the complete results of zero-shot cross-modal retrieval, comparing SensorLM to LLM baselines. Evaluations are conducted on query-target sets of size 100, 5k, and 40k, using Recall@1, Recall@5, and Recall@10 (R@K). These metrics capture the proportion of queries where the correct target appears among the top K retrieved results.

SensorLM consistently demonstrates strong retrieval performance across all settings and directions. Notably, it achieves perfect 100% recall at R@1, R@5, and R@10 on the 100-sample benchmark for both Sensor → Text and Text → Sensor retrieval. Even at the 40k scale, SensorLM maintains high accuracy, with R@1 scores of 96.1% for Sensor → Text and 90.0% for Text → Sensor.

In contrast, the LLM baselines are largely unable to perform most retrieval tasks due to context length limitations, marked as “–” in the table. Where results are available (mainly for the 100-sample set), their performance is significantly lower than SensorLM. These findings highlight SensorLM’s superior capability in cross-modal retrieval, where general-purpose LLMs struggle without domain-specific

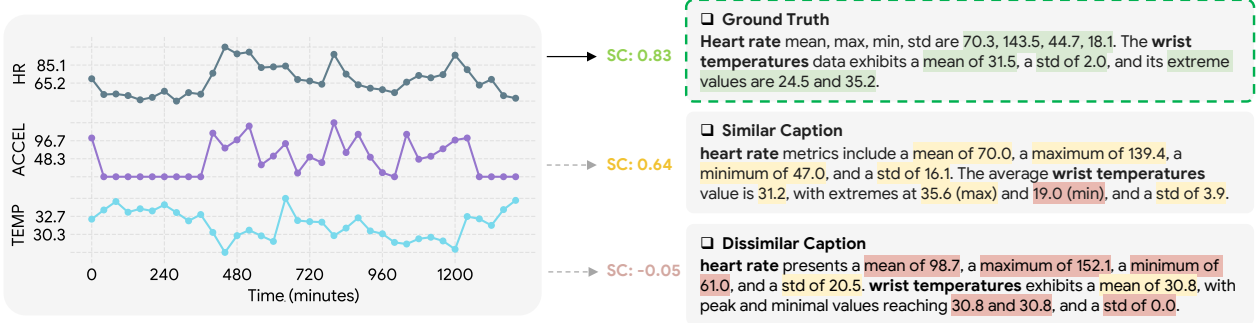


Figure 10 | Zero-shot sensor-to-text retrieval qualitative example for statistical captions. We show similarity scores (SC) for the correctly retrieved ground truth, a top similar caption, and a dissimilar caption. Green highlights correct statistics; Yellow indicates close matches; and Red denotes distinctly different stasistics. In addition to correctly retrieving the ground truth, SensorLM also demonstrates semantic understanding by assigning high similarity scores to numerically closer candidates.

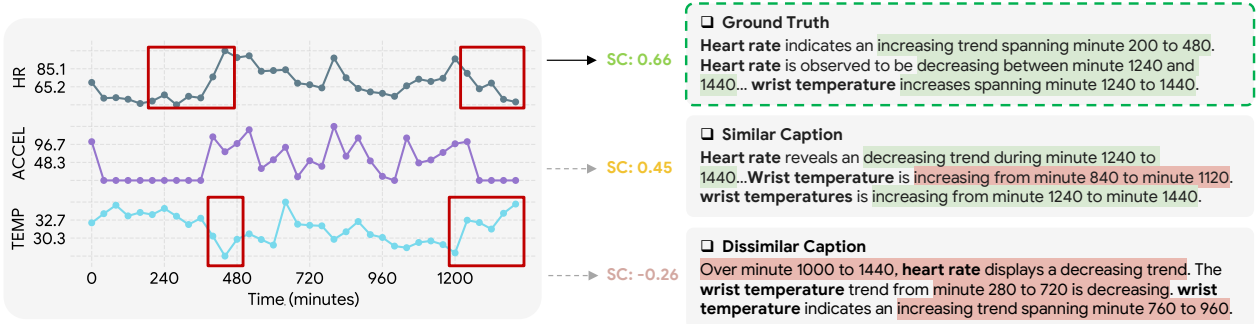


Figure 11 | Zero-shot sensor-to-text retrieval qualitative example for structural captions. We show similarity scores (SC) for the correctly retrieved ground truth, a top similar caption, and a dissimilar caption. Green highlights correct patterns and time frames; Yellow indicates partial matches; and Red denotes incorrect patterns and time frames. In addition to correctly retrieving the ground truth, SensorLM also demonstrates semantic understanding by assigning high similarity scores to partially correct candidates.

architectural adaptations or training.

In addition to the *semantic* caption example in Fig. 4, Fig. 10 provides qualitative evidence of SensorLM’s ability to retrieve accurate *statistical* summaries from raw sensor inputs. SensorLM retrieves the ground-truth caption as well as similar alternatives that match sensor statistics (highlighted in yellow), such as means, standard deviations, and extreme values. In contrast, unrelated captions show low similarity scores, reflecting SensorLM’s understanding of the statistical structure of the data.

Furthermore, Fig. 11 illustrates SensorLM’s capacity for retrieving *structural* descriptions from sensor data. It accurately identifies the ground-truth structural caption and retrieves similar captions that describe temporal dynamics, such as trends and spike events. This demonstrates SensorLM’s ability to interpret and express dynamic temporal features within sensor signals.

C.4. Caption Generation

Table 22 evaluates sensor caption generation performance, comparing SensorLM against LLM baselines. We report standard Natural Language Generation (NLG) metrics: BERTScore (Precision, Recall, F1), METEOR, and ROUGE, which collectively assess semantic similarity, fluency, and content overlap.

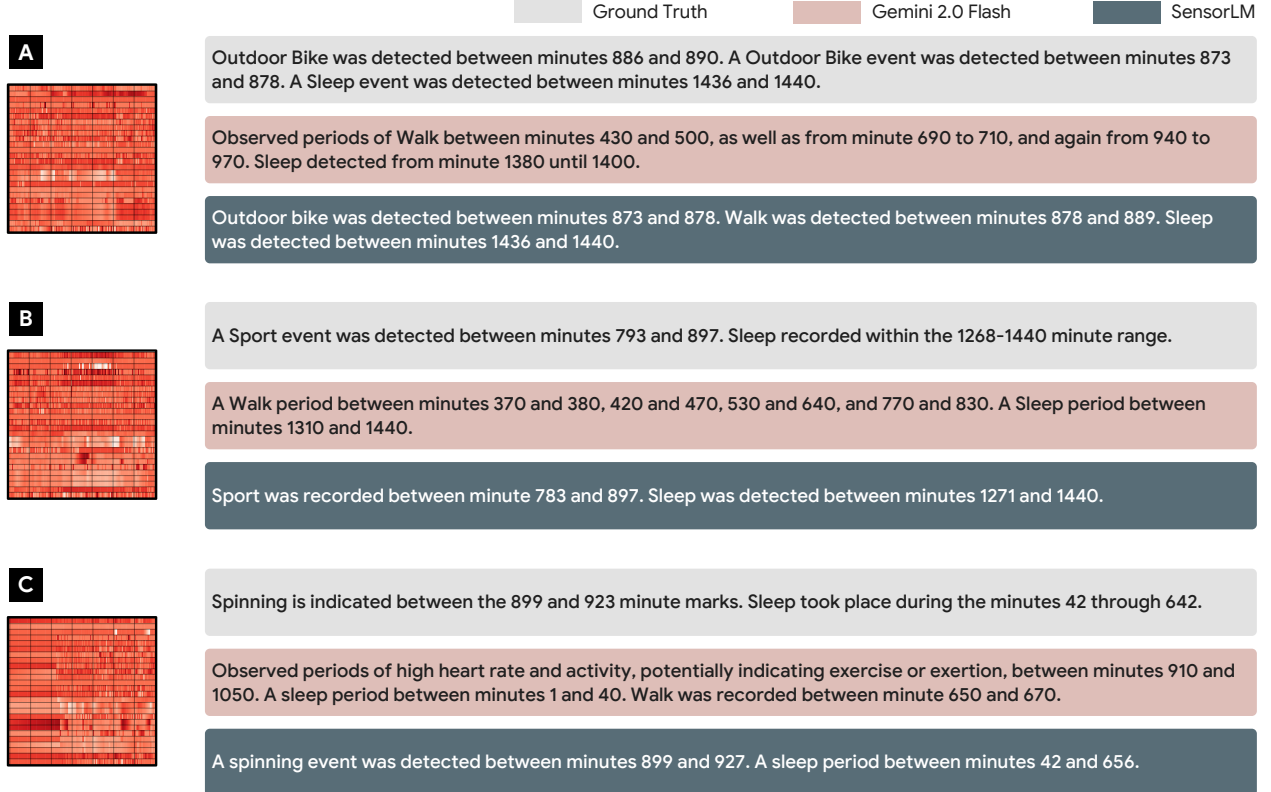


Figure 12 | Qualitative comparison of sensor caption generation between Gemini 2.0 Flash and SensorLM against ground truth. We show various examples of *semantic caption* generation from wearable sensor inputs. Compared to the baseline, SensorLM demonstrates stronger semantic understanding by generating coherent events with near-correct localized timeframes.

Table 22 | Sensor caption generation results. We compare SensorLM with LLM baselines using commonly adopted metrics (e.g., BERTScore, METEOR, ROUGE) for natural language generation.

Metrics	BERT Score				
	Precision \uparrow	Recall \uparrow	F1 \uparrow	METEOR \uparrow	ROUGE \uparrow
Gemma-3-27B [29]	0.82	0.85	0.83	0.19	0.11
Gemini 2.0 [28]	0.86	0.87	0.86	0.26	0.20
SensorLM	0.93	0.91	0.92	0.33	0.40

SensorLM consistently outperforms both LLM baselines across all metrics.

We also present three qualitative examples in Fig. 12, which compare sensor caption outputs from Gemini 2.0 Flash and SensorLM against ground truth references. The examples focus on *semantic caption* generation from wearable sensor inputs. Compared to the baseline, SensorLM demonstrates stronger semantic understanding by generating coherent event descriptions with accurately localized timeframes.

Table 23 | **Comparisons of SensorLM caption versions.** We evaluate different combinations of caption types used during pretraining. AUROC \uparrow is used as the metric. Best results of each column are in **bold** and the second best are underlined. Default setting used in the main experiments is marked in gray .

Caption Variant	Zero-Shot		Linear Probing		Retrieval (40k)
	Activity	Activity	Anxiety	Hypertension	Recall@1
statistical	0.51	0.76	<u>0.67</u>	0.63	1.00
structural	0.50	0.78	0.63	0.59	1.00
semantic	<u>0.71</u>	0.95	0.65	0.60	0.89
statistical + semantic	0.66	0.84	0.68	<u>0.62</u>	1.00
structural + semantic	0.84	0.94	0.65	0.60	1.00
statistical + structural	0.49	0.79	<u>0.67</u>	0.63	0.64
statistical + structural + semantic	0.66	0.86	0.68	0.63	0.90

Table 24 | **Comparisons of SensorLM architectural variants.** We compare different choices used during pretraining. Default setting used in the main experiments is marked in gray .

Metrics	Zero-Shot			Linear Probing		
	AUROC \uparrow	F1 \uparrow	Balanced Acc. \uparrow	AUROC \uparrow	F1 \uparrow	Balanced Acc. \uparrow
SensorLM (CLIP)	0.83	0.29	0.31	0.93	0.53	0.55
SensorLM (Cap)	0.55	0.01	0.05	0.90	0.32	0.52
SensorLM (CoCa)	0.84	0.29	0.32	0.94	0.57	0.60

C.5. Complete Ablation Results

Here we present the complete results for the ablation studies introduced in Sec. 5.3. Table 23 examines how different combinations of sensor caption types (*statistical*, *structural*, and *semantic*) affect SensorLM’s performance across downstream tasks. Semantic captions are critical for zero-shot activity recognition, while combining them with structural captions further enhances performance across tasks, including cross-modal retrieval. The results also reveal trade-offs: statistical captions improve performance on “Anxiety” and “Hypertension”, but slightly reduce accuracy on “Activity”.

Table 24 evaluates different architectural variants of SensorLM during pretraining. SensorLM (CoCa) consistently outperforms single-objective variants (SensorLM (CLIP) and SensorLM (Cap)) across key metrics for both zero-shot classification and linear probing, validating the benefits of integrating contrastive and generative objectives.

D. Societal Impact

Broader Impacts. Ubiquitous health technologies, particularly wearables, offer tremendous potential to transform healthcare through continuous, longitudinal personal monitoring. However, the complexity of raw sensor data often restricts insights to low-level metrics. SensorLM addresses this challenge by translating multimodal sensor signals into natural language, enabling a more intuitive and accessible interface for both consumers and domain experts. This capability promotes clearer,

more actionable insights, potentially fostering more proactive, personalized, and preventative health management.

Limitations and Ethical Considerations. While consumer health research holds great promise, it must be guided by careful attention to safety, fairness, and privacy. The possibility of misuse by malicious actors underscores the importance of responsible development. Although we advocate for open science, health data—by its nature—requires a delicate balance between research reproducibility and participant confidentiality.

Importantly, SensorLM is a research prototype and is not intended for clinical use. It has not been validated as a diagnostic tool and should not be used for medical decision-making without formal regulatory approval. Clinical deployment would necessitate rigorous validation and compliance with relevant healthcare regulations.

Finally, while SensorLM’s methodology is designed to be generalizable, our current evaluation is limited to specific wearable devices and sensor modalities. Further research is needed to assess its performance across broader device ecosystems, data modalities, and population groups.